

Contrasting effects of acidification and warming on dimethylsulfide concentrations during a temperate estuarine fall bloom mesocosm experiment

Robin Bénard¹, Maurice Levasseur¹, Michael Scarratt², Sonia Michaud², Michel Starr², Alfonso Mucci³, Gustavo Ferreyra^{4,5}, Michel Gosselin⁴, Jean-Éric Tremblay¹, Martine Lizotte¹, Gui-Peng Yang⁶

¹Département de biologie, Université Laval, 1045 avenue de la Médecine, Québec, Québec G1V 0A6, Canada

²Fisheries and Oceans Canada, Maurice Lamontagne Institute, P.O. Box 1000, Mont-Joli, Québec G5H 3Z4, Canada

³Department of Earth and Planetary Sciences, McGill University, 3450 University Street, Montréal, Québec H3A 2A7, Canada

⁴Institut des sciences de la mer de Rimouski (ISMER), Université du Québec à Rimouski, 310 allée des Ursulines, Rimouski, Québec G5L 3A1, Canada

⁵Centro Austral de Investigaciones Científicas (CADIC), Consejo Nacional de Investigaciones Científicas y Técnicas, Bernardo Houssay 200, 9410 Ushuaia, Tierra del Fuego, Argentina

⁶Institute of Marine Chemistry, Ocean University of China, 238 Songling Road, Qingdao 266100, Shandong, China

Correspondence: Robin Bénard (robin.benard.1@ulaval.ca)

Abstract. The effects of ocean acidification and warming on the concentrations of dimethylsulfoniopropionate (DMSP) and dimethylsulfide (DMS) were investigated during a mesocosm experiment in the Lower St. Lawrence Estuary (LSLE) in the fall of 2014. Twelve mesocosms covering a range of pH_T (pH on the total hydrogen ion concentration scale) from 8.0 to 7.2, corresponding to a range of CO_2 partial pressures (pCO_2) from 440 to 2900 μatm , at two temperatures (in situ and +5 °C; 10 °C and 15 °C) was monitored during 13 days. All mesocosms were characterized by the rapid development of a diatom bloom dominated by *Skeletonema costatum*, followed by its decline upon the exhaustion of nitrate and silicic acid. Neither the acidification nor the warming resulted in a significant impact on the abundance of bacteria over the experiment. However, warming the water by 5 °C resulted in a significant increase of the average bacterial production (BP) in all 15 °C mesocosms as compared to 10 °C, with no detectable effect of pCO_2 on BP. Variations in total DMSP ($\text{DMSP}_t = \text{particulate} + \text{dissolved DMSP}$) concentrations tracked the development of the bloom although the rise in DMSP_t persisted for a few days after the peaks in chlorophyll *a*. Average concentrations of DMSP_t were not affected by acidification or warming. Initially low concentrations of DMS (< 1 nmol L^{-1}) increased to reach peak values ranging from 30 to 130 nmol L^{-1} towards the end of the experiment. Increasing the pCO_2 reduced the averaged DMS concentrations by 66 % and 69 % at 10 °C and 15 °C, respectively, over the duration of the experiment. On the other hand, a 5 °C warming increased DMS concentrations by an average of 240 % as compared to in situ temperature, resulting in a positive offset of the adverse pCO_2 impact. Significant positive correlations found between bacterial production and concentrations of DMS throughout our experiment point towards temperature-associated enhancement of bacterial DMSP metabolism as a likely driver for the mitigating effect of warming on the negative impact of acidification on the net production of DMS in the LSL and potentially the global ocean.

35 1. Introduction

36 Dimethylsulfide (DMS) is ubiquitous in productive estuarine, coastal, and oceanic surface waters (Barnard et al., 1982;
37 Iverson et al., 1989; Kiene and Service, 1991; Cantin et al., 1996; Kettle et al., 1999). With an estimated average 28.1 Tg of
38 sulfur (S) being transferred to the atmosphere annually (Lana et al., 2011), DMS emissions constitute the largest natural
39 source of tropospheric S (Lovelock et al., 1972; Andreae 1990; Bates et al., 1992). The oxidation of atmospheric DMS yields
40 hygroscopic sulfate (SO_4^{2-}) aerosols that directly scatter incoming solar radiation and act as nuclei upon which cloud droplets
41 can condense and grow, thereby potentially impacting cloud albedo and the radiative properties of the atmosphere (Charlson
42 et al., 1987; Andreae and Crutzen 1997; Liss and Lovelock, 2007; Woodhouse et al., 2013). The scale of the impact of
43 biogenic SO_4^{2-} particles on global climate, however, remains uncertain (Carslaw et al., 2010; Quinn and Bates, 2011, Quinn
44 et al., 2017). The strength of DMS emissions depends on wind- and temperature-driven transfer processes (Nightingale et al.,
45 2000) but mostly on its net production in the surface mixed layer of the ocean (Malin and Kirst, 1997). Net changes in the
46 aqueous DMS inventory are largely governed by microbial food webs (see reviews by Simó, 2001; Stefels et al., 2007)
47 whose productivity is potentially sensitive to modifications in the habitats that sustain them. Given the complexity of the
48 biological cycling of DMS, understanding how climate change related stressors could impact the production of this climate-
49 active gas is a worthy but formidable challenge.

50 DMS is produced, for the most part, from the enzymatic breakdown of dimethylsulfoniopropionate (DMSP) (Cantoni and
51 Anderson, 1956), a metabolite produced by several groups of phytoplankton, with an extensive range in intracellular quotas
52 between taxa (Keller et al., 1989; Stefels et al., 2007). Several species of the classes Haptophyceae and Dinophyceae are
53 amongst the most prolific DMSP producers, but certain members of Bacillariophyceae (diatoms) and Chrysophyceae can
54 also produce significant amounts of DMSP (Stefels et al., 2007). The biosynthesis of DMSP is highly constrained by abiotic
55 factors and its up- or down-regulation may allow cells to cope with environmental shifts in temperature, salinity, nutrients
56 and light intensity (Kirst et al., 1991; Karsten et al., 1996; Sunda et al., 2002), while its de novo synthesis and exudation may
57 also serve as a sink for excess carbon (C) and sulfur (S) under unfavourable growth conditions (Stefels, 2000). Beyond
58 active exudation in healthy cells (Laroche et al., 1999), cellular or particulate DMSP (DMSP_p) can be transferred to the water
59 column as dissolved DMSP (DMSP_d) through viral lysis (Hill et al., 1998; Malin et al., 1998), autolysis (Nguyen et al., 1988;
60 Stefels and Van Boeckel, 1993), and grazing by micro-, meso- and macrozooplankton (Dacey and Wakeham, 1986; Wolfe
61 and Steinke, 1996). The turnover rate of DMSP_d in the water column is generally very rapid (a few hours to days) as this
62 compound represents sources of C and reduced S for the growth of microbial organisms (Kiene and Linn, 2000).
63 Heterotrophic bacteria mediate most of the turnover of S- DMSP_d through pathways that constrain the overall production of
64 DMS: (1) enzymatic cleavage of DMSP_d that yields DMS; (2) demethylation/ demethiolation of DMSP_d that yields
65 methanethiol (MeSH); (3) production of dissolved non-volatile S compounds, including SO_4^{2-} , following oxidation of
66 DMSP_d ; (4) intracellular accumulation of DMSP_d with no further metabolization (Kiene et al., 1999, 2000; Kiene and Linn,
67 2000; Yoch, 2002). A compilation of ^{35}S - DMSP_d tracer studies conducted with natural microbial populations shows that

68 microbial DMS yields rarely exceed 40% of consumed DMSP_d in surface coastal and oceanic waters (see review table in
69 Lizotte et al., 2017). Another potential fate of DMSP_d is its uptake by non-DMSP producing eukaryotic phytoplankton such
70 as certain diatoms (Vila-Costa et al., 2006b; Ruiz-González et al., 2012) and cyanobacteria such as *Synechococcus* and
71 *Prochlorococcus* (Malmstrom et al., 2005; Vila-Costa et al., 2006b), but the overall turnover of DMSP_d seems to be
72 dominated by heterotrophic organisms.

73 Whereas the role of bacteria in the production of DMS via DMSP_d is well recognized, an increasing number of studies have
74 shown that the phytoplankton-mediated enzymatic conversion of total DMSP (DMSP_t) into DMS can also be significant
75 when communities are dominated by DMSP-lyase producing phytoplankton groups such as Dinophyceae and Haptophyceae
76 (Niki et al., 2000; Steinke et al., 2002; Stefels et al., 2007; Lizotte et al., 2012), particularly under high doses of solar
77 radiation (Toole and Siegel, 2004; Toole et al., 2006, 2008; Vallina et al., 2008). Removal processes of DMS from surface
78 waters include photo-oxidation, bacterial degradation, and efflux across the air-sea interface which individually depends on
79 several factors such as light intensity, wind velocity, the depth of the surface mixed layer, and the gross production of DMS
80 (Brimblecombe and Shooter, 1986; Simó and Pedros-Alió, 1999; Nightingale et al., 2000; Hatton et al., 2004; Simó, 2004).
81 Additionally, the biological and photochemical oxidation of dimethylsulfoxide (DMSO) is an important sink for DMS, while
82 DMSO reduction represents a DMS source (Stefels et al. 2007; Spiese et al., 2009; Asher et al., 2011). Overall, production
83 and turnover of DMS and its precursor DMSP are unequivocally linked with microbial activity, both autotrophic and
84 heterotrophic. The associated biological processes and interactions amongst these microorganisms have been shown to be
85 sensitive to fluctuations in abiotic factors and may thus be further modulated by multiple drivers of climate change.

86 Since the pre-industrial era, atmospheric CO₂ concentrations have risen from 280 ppm, and, according to the results of the
87 global ocean circulation models under the condition of the business-as-usual scenario RCP 8.5, are expected to reach 850–
88 1370 ppm by 2100 (IPCC, 2013). The oceans have already absorbed about 28 % of the anthropogenic CO₂ emitted to the
89 atmosphere (Le Quéré et al., 2015), leading to a pH decrease of 0.11 units in surface waters (Gattuso et al., 2015), a
90 phenomenon called ocean acidification (OA). An additional decrease of pH by 0.3–0.4 units is expected by the end of this
91 century, and could reach 0.8 units by 2300 (Caldeira and Wickett, 2005; Doney et al., 2009; Feely et al., 2009). In addition to
92 the oceanic sink, a similar fraction of anthropogenic CO₂ emissions has been captured by terrestrial vegetation, while the
93 anthropogenic CO₂ remaining (45% of total emissions) in the atmosphere (Le Quéré et al., 2013) has led to an estimated
94 increased greenhouse effect of 0.3–0.6 W m⁻² globally over the past 135 years (Roemmich et al., 2015). Ninety percent of
95 this excess heat has been absorbed by the ocean, increasing sea surface temperatures (SST) ~0.1 °C per decade since 1951
96 and could increase SST by 3–5 °C before 2100 (IPCC, 2013). Leading experts in the field of global change have called upon
97 the scientific community to address critical knowledge gaps, among which, a top priority remains the assessment of the
98 impact of multiple environmental stressors on marine microorganisms (Riebesell and Gattuso, 2015).

99 The sensitivity of natural planktonic assemblages to OA, along with their production of DMSP and DMS, has been
100 investigated in several experimental studies (see review table in Husserr et al., 2017). The majority of these experiments
101 have shown a decrease in both DMSP and DMS concentrations with increasing pCO₂ (Hopkins et al., 2010; Avgoustidi et

102 al., 2012; Park et al., 2014; Webb et al., 2015). The decrease in DMSP production has largely been attributed to the
103 deleterious impact of decreasing pH on the coccolithophore *Emiliania huxleyi*, the dominant DMSP producer in several of
104 these studies. Nevertheless, OA does not always result in a concomitant decrease in DMSP and DMS production. For
105 example, the pCO₂-induced decrease in DMS reported by Archer et al. (2013) in Arctic waters was accompanied by an
106 increase in DMSP concentrations, indicating that DMS production is at least partly dependent on the turnover of DMSP,
107 rather than on the DMSP pool. A modeling study showed that the specific implementation of the negative effect of OA on
108 DMS net production in a coupled ocean-atmosphere model reduces global DMS production by 18 ± 3 %, resulting in an
109 additional warming of 0.23–0.48 K by 2100 under the A1B scenario (Six et al., 2013). Schwinger et al. (2017) further
110 showed that the OA-induced decreases in oceanic DMS emissions could result in a transient global warming of 0.30 K,
111 mostly resulting from a reduction of cloud albedo. These first attempts to model the potential effect of OA on climate
112 through its impact on DMS oceanic production show that OA may significantly affect climate by reducing marine emissions
113 of DMS but also highlight the importance of carefully assessing the robustness of the DMS-OA negative relationship. This is
114 particularly relevant considering that some experiments reveal a neutral or positive effect of increasing pCO₂ on DMS net
115 production (Vogt et al., 2008; Kim et al., 2010; Hopkins and Archer, 2014). Regional or seasonal differences in
116 phytoplankton taxonomy, microzooplankton grazing, and bacterial activity have been proposed as key drivers of the
117 discrepancies between these experimental results.

118 Whereas studies of the impact of OA on DMS cycling have gained momentum, the importance of assessing how combined
119 drivers of change may impact the structure and the functioning of ocean ecosystems, using multifactorial approaches, is now
120 increasingly recognized (Boyd et al., 2015; 2018; Riebesell and Gattuso, 2015; Gunderson et al., 2016). Thus far, only two
121 mesocosm studies assessed the combined effect of OA and warming on DMS dynamics by natural plankton assemblages.
122 The two studies, both conducted with coastal waters, led to contrasting results. The first study showed an 80 % increase in
123 DMS concentrations under high pCO₂ conditions (900 ppm vs. 400 ppm), and a reduction by 20 % of this stimulating effect
124 when the increase in pCO₂ was accompanied by a 3 °C warming (Kim et al., 2010). However, the absence of a specific
125 stand-alone warming treatment did not allow the authors to assess the sole impact of temperature on DMS net production.
126 The second study showed decreasing DMS concentrations under both acidification and greenhouse conditions, with the
127 lowest DMS concentrations measured under combined acidification and warming treatments (Park et al., 2014). The authors
128 attributed these contrasting responses to differences in the phytoplankton assemblages, DMSP-related algal physiological
129 characteristics, and microzooplankton grazing. Nevertheless, questions remain as to the combined effect of pCO₂ and
130 warming on DMS net production since the temperature treatments were not conducted over the full range of pCO₂ tested
131 (Kim et al., 2010; Park et al., 2014).

132 The combined influence of acidification and warming on the dynamics of the St. Lawrence Estuary phytoplankton fall bloom
133 was investigated during a full factorial mesocosm experiment (Bénard et al., 2018). During this experiment, a bloom of
134 *Skeletonema costatum* developed in all mesocosms, independently of the pCO₂ gradient (from 440 to 2900 µatm) and
135 temperatures tested (10 and 15 °C). The increase in pCO₂ had no influence on the bloom but warming accelerated the growth

136 rate of the diatoms and hastened the decline of the bloom (Bénard et al., 2018). Here, we report on the impacts of
137 acidification and warming on DMSP and DMS concentrations with a focus on the dynamics of heterotrophic bacteria, a
138 component of the marine food web known to affect the turnover of DMSP and DMS.

139 **2. Materials and methods**

140 **2.1 Mesocosm setup**

141 The mesocosm experimental setup is described in detail in Bénard et al. (2018). Briefly, mesocosm experiments were
142 conducted at the ISMER marine research station of Rimouski (Québec, Canada) in the fall of 2014. The twelve 2600 L
143 cylindrical (2.67 m × 1.4 m), conical bottom, mesocosms were housed in two temperature-controlled, full-size shipping
144 containers each containing six mesocosms (Aquabiotech Inc., Québec, Canada). Each mesocosm is mixed by a propeller
145 secured near the top of the enclosure to ensure homogeneity of the water column. The mesocosms are sealed by a Plexiglas
146 cover transmitting 50–85 % of solar UVB (280–315 nm), 85–90 % of UVA (315–400 nm), and 90 % of photosynthetically
147 active radiation (PAR; 400–700 nm) of the natural incident light. Independent temperature probes (AQB-Temperature
148 sensor, accuracy ± 0.2 °C) were installed in each mesocosm, recording temperature every 15 minutes and either triggering a
149 resistance heater (Process Technology TTA1.8215) or a glycol refrigeration system activated by an automated pump. The pH
150 of the mesocosms was measured every 15 minutes by Hach® PD1P1 probes (± 0.02 pH units) linked to Hach® SC200
151 controllers. To maintain pH, two reservoirs of artificial seawater were equilibrated with pure CO₂ before the start of the
152 experiment and positive deviations from the target pH values in each mesocosm activated peristaltic pumps that injected the
153 CO₂ supersaturated seawater into the mesocosm water. This control system was able to maintain the pH in the mesocosms
154 within ± 0.02 pH units of the targeted values during the initial bloom development by lowering the pH, but it could not
155 increase the pH during the declining phase of the bloom.

156 **2.2 Experimental approach**

157 Prior to the onset of the experiment, all the mesocosms were meticulously washed with diluted Virkon™, an anti-viral and
158 anti-bacterial solution, according to the manufacturer's instructions (Antec International Limited), and thoroughly rinsed.
159 The experimental approach is also detailed in Bénard et al. (2018). To fill the mesocosms, water from ~5 m depth was
160 collected near the Rimouski harbour (48° 28' 39.9" N, 68° 31' 03.0" W) on the 27th of September 2014 (day -5). Initial
161 conditions were: practical salinity (S_p) = 26.52, temperature = 10 °C, nitrate (NO_3^-) = $12.8 \pm 0.6 \mu\text{mol L}^{-1}$, silicic acid
162 (Si(OH)_4) = $16 \pm 2 \mu\text{mol L}^{-1}$, and soluble reactive phosphate (SRP) = $1.4 \pm 0.3 \mu\text{mol L}^{-1}$. Following its collection, the water
163 was screened through a 250 μm mesh while the mesocosms were simultaneously gravity-filled by a custom made “octopus”
164 tubing system. The initial in situ temperature of 10 °C was maintained in all mesocosms for the first 24 h (day -4). On day -
165 3, the six mesocosms in one of the containers were gradually heated to 15 °C while the mesocosms in the other container
166 were maintained at 10 °C. No manipulations were performed on day -2 to avoid excessive stress, and acidification was

167 carried out on day -1. The mesocosms were initially set to cover a gradient of pH_T (total proton concentration scale) of ~8.0
168 to 7.2 corresponding to a range of pCO_2 from 440 to 2900 μatm . Two mesocosms, one in each container (at each
169 temperature), were not pH-controlled to assess the effect of freely fluctuating pH condition. These two mesocosms were
170 called drifters since the in-situ pH was allowed to drift over time throughout the bloom development. To achieve the initially
171 targeted pH_T , CO_2 -saturated artificial seawater was added to mesocosms M1, M3, M5, M7, M8, M10 (pH_T 7.2–7.6) while
172 mesocosms M2, M4, M6, M9, M11, M12 (pH_T 7.8–8.0 and the drifters) were openly mixed to allow CO_2 degassing. Then,
173 the automatic system controlling the occasional addition of CO_2 -saturated artificial seawater maintained the pH equal or
174 below the targeted pH, except for the drifters.

175 **2.3 Seawater analysis**

176 Daily sampling of the mesocosms was carried out between 05:00 and 08:00 every day (EDT) as described in Bénard et al.
177 (2018). Samples for carbonate chemistry, nutrients, DMSP and DMS were collected directly from the mesocosms prior to
178 filling of 20 L carboys from which seawater for the determination of chlorophyll *a* (Chl *a*), bacterial abundance, and
179 bacterial production (BP) was subsampled. Samples were collected directly from the mesocosms and the artificial seawater
180 tank on days -3, 3 and 13 for practical salinity determinations. The samples were collected in 250 mL plastic bottles and
181 stored in the dark until analysis was carried out on a Guildline Autosol 8400B salinometer in the months following the
182 experiment.

183 **2.3.1 Carbonate chemistry and nutrients**

184 Analytical methods used to determine the carbonate parameters are described in detail in Bénard et al. (2018). Briefly, pH
185 was determined every day by transferring samples from the mesocosms to 125 mL plastic bottles without headspace. The
186 samples were analyzed within hours of collection on a Hewlett-Packard UV-Visible diode array spectrophotometer (HP-
187 8453A) and a 5 cm quartz cell using phenol red (PR; Robert-Baldo et al., 1985) and *m*-cresol purple (mCP; Clayton and
188 Byrne, 1993) as indicators after equilibration to 25.0 ± 0.1 °C in a thermostated bath. The pH on the total proton scale (pH_T)
189 was calculated according to Byrne (1987), with the salinity of the sample and the HSO_4^- association constants given by
190 Dickson (1990). The reproducibility of pH measurements, based on replicate measurements of the same samples and values
191 derived from both indicators, was on the order of 0.003. Samples for total alkalinity (TA) were collected every 3–4 days in
192 250 mL glass bottles to which a few crystals of HgCl_2 were added before sealing with ground glass stoppers and Apiezon[®]
193 Type-M high-vacuum grease. The TA determinations were carried out within one day of sampling by open-cell automated
194 potentiometric titration (Titralab 865, Radiometer[®]) with a pH combination electrode (pHC2001, Red Rod[®]) and a dilute
195 (0.025 M) HCl titrant solution calibrated against Certified Reference Materials (CRM Batch#94, provided by A. G. Dickson,
196 Scripps Institute of Oceanography, La Jolla, USA). The average relative error, calculated from the average relative standard
197 deviation on replicate standards and sample analyses, was < 0.15 %. The computed pH_T at 25 °C, measured TA, silicic acid

198 and SRP concentrations were used to calculate the in situ pH_T , pCO_2 and saturation state of the water in each mesocosm
199 using CO₂SYS (Pierrot et al., 2006) and the carbonic acid dissociation constants of Cai and Wang (1998).
200 The samples for the determination of NO_3^- , $Si(OH)_4$, and SRP were filtered through Whatman GF/F filters, collected in acid
201 washed polyethylene tubes and stored at -20 °C. Analysis was carried out using a Bran and Luebbe Autoanalyzer III using
202 the colorimetric methods of Hansen and Koroleff (2007). The analytical detection limit was 0.03 $\mu mol L^{-1}$ for NO_3^- plus
203 nitrite (NO_2^-), 0.02 $\mu mol L^{-1}$ for NO_2^- , 0.1 $\mu mol L^{-1}$ for $Si(OH)_4$, and 0.05 $\mu mol L^{-1}$ for SRP.

204 2.3.2 Biological variables

205 Chl *a* determination methods are presented in B nard et al. (2018). Succinctly, duplicate 100 mL samples were filtered onto
206 Whatman GF/F filters. The filters were soaked in a 90 % acetone solution at 4 °C in the dark for 24 h, the solution was then
207 analyzed by a 10-AU Turner Designs fluorometer (acidification method: Parsons et al., 1984). The analytical detection limit
208 for Chl *a* was 0.05 $\mu g L^{-1}$.

209 Samples for the determination of free-living heterotrophic bacteria were kept in sterile cryogenic polypropylene vials and
210 fixed with glutaraldehyde Grade I (final concentration = 0.5 %, Sigma Aldrich; Marie et al., 2005). Duplicate samples were
211 placed at 4 °C in the dark for 30 min, then frozen at -80 °C until analysis by a FACS Calibur flow cytometer (Becton
212 Dickinson) equipped with a 488 nm argon laser. Before enumeration, the samples were stained with SYBR Green I (0.1 %
213 final concentration, Invitrogen Inc.) to which 600 μl of a Tris-EDTA 10 \times buffer of pH 8 were added (Laboratoire MAT;
214 Belzile et al., 2008). Fluoresbrite beads (diameter 1 μm , Polysciences) were also added to the sample as an internal standard.
215 The green fluorescence of SYBR Green I was measured at 525 ± 5 nm. Bacterial abundance was determined as the sum of
216 low and high nucleic (LNA and HNA) counts (Annane et al., 2015).

217 Bacterial production was estimated in each mesocosm except the drifters on days 0, 2, 4, 6, 8, 10, 11 and 13 by measuring
218 incorporation rates of tritiated thymidine (3H -TdR), using an incubation and filtration protocol based on Fuhrman and Azam
219 (1980, 1982). Twenty mL water subsamples were transferred from glass Erlenmeyers to five sterile glass vials; three as
220 “measured” values and two as blanks. In all blank vials, 0.2 mL of formaldehyde 37 % were added, immediately after the
221 sampling to stop all biological activities. Then, 1 mL of 3H -TdR solution (4 $\mu mol L^{-1}$), prepared from commercial solution
222 (63 Curie $mmol^{-1}$; 1 mCurie mL^{-1} , 10 $\mu mol L^{-1}$ 3H -TdR, MP Biomedicals), was added in all vials. Samples were incubated
223 2.5 h at experimental temperatures (10 or 15 °C), and then 0.2 mL of formaldehyde 37 % were immediately added in the
224 three “measure” vials. Bacteria were then collected by filtration (diameter 25 mm; 0.2 μm porosity) and filters were treated
225 according to Fuhrman and Azam (1980, 1982). 3H -TdR incorporation was measured using a scintillation counter (Beckman
226 LS5801) and results were expressed in dpm. Blank values were subtracted from “measured” values to remove background
227 radioactivity. 3H -TdR incorporation rates were converted in mole of 3H -TdR incorporated per unit of volume and time,
228 before converting to rate of carbon production using the carbon conversion factor of Bell (1993).

229 **2.3.3 DMSP and DMS concentrations**

230 For the quantification of DMSP_t, duplicate 3.5 mL samples of seawater were collected into 5 mL polyethylene tubes.
231 Samples were preserved by adding 50 µL of a 50 % sulfuric acid solution (H₂SO₄) to the tubes before storage at 4 °C in the
232 dark until analysis in the following months. Samples for the quantification of DMSP_d were taken daily, but a technical
233 problem during storage and transport of the samples led to a loss of all samples. To quantify DMSP_t, 1 mL of NaOH (5 M)
234 was injected into a purge and trap (PnT) system prior to the 3.5 mL sample to hydrolyze DMSP into DMS following a mole-
235 to-mole conversion. Ultrapure helium was used to bubble the heated chamber (70 °C; 50 ± 5 mL min⁻¹; 4 min) trapping the
236 gas sample in a loop immersed in liquid nitrogen. The loop was then heated in a water bath to release the trapped sample and
237 analyzed using a Varian 3800 Gas Chromatograph equipped with a pulsed flame photometric detector (PFPD, Varian 3800)
238 and a detection limit of 0.9 nmol L⁻¹ (Scarratt et al., 2000; Lizotte et al., 2012). DMSP concentrations were determined
239 against a calibration curve using standardized DMSP samples prepared by diluting known concentrations of DMSP standard
240 (Research Plus Inc.) into deionized water and analyzed following the same methodology.

241 Samples for the quantification of DMS were directly collected from the mesocosms into 20 mL glass vials with a butyl septa
242 and aluminum crimp. The samples were kept in the dark at 4 °C until analysis was carried out within hours of collection by
243 injecting the 20 mL sample in the PnT system described above, without the prior addition of NaOH. DMS concentrations
244 were calculated against microliter injections of DMS diluted with ultrapure helium using a permeation tube (Certified
245 Calibration by Kin-Tek Laboratories Inc.; Lizotte et al., 2012).

246 **2.4 Statistical analyses**

247 The statistical analyses were performed using the nlme package in R (R Core Team, 2016). The data were analyzed using a
248 general least squares (gls) approach to test the linear effects of the two treatments (temperature, pCO₂), and their interaction
249 on the variables (Paul et al., 2016; Hussherr et al., 2017; Bénard et al., 2018). The analyses were conducted on the averages
250 of the measured parameters over the whole duration of the experiment, and separate regressions for pCO₂ were performed
251 for each temperature when the latter had a significant effect. The residuals were checked for normality using a Shapiro-Wilk
252 test ($p > 0.05$) and data were transformed (square root or natural logarithm) if necessary. In addition, squared Pearson's
253 correlation coefficients (r^2) with a significance level of 0.05 were used to evaluate correlations between key variables.

254 **3. Results**

255 **3.1 Physical and chemical conditions during the experiments**

256 The S_p was 26.52 ± 0.03 on day -4 in all mesocosms and remained constant throughout the experiment, averaging
257 26.54 ± 0.02 on day 13 (Bénard et al., 2018). The temperature of the mesocosms in each container remained within ± 0.1 °C
258 of the target temperature throughout the experiment and averaged 10.04 ± 0.02 °C for mesocosms M1 through M6, and

259 15.0 ± 0.1 °C for mesocosms M7 through M12 (Fig. 1a). The pH_T remained relatively stable throughout the experiment in
260 the pH-controlled treatments, but decreased slightly as the experiment progressed, deviating by an average of -0.14 ± 0.07
261 units relative to the target pH_T on the last day (Fig. 1b). The pH variations corresponded to changes in pCO₂ from an average
262 of 1340 ± 150 µatm on day -3, and ranged from 564 to 2902 µatm at 10 °C and from 363 to 2884 µatm at 15 °C on day 0
263 following the acidification (Fig. 1c). The in situ pH_T in the drifters (M6 and M11) increased from 7.896 and 7.862 on day 0,
264 at 10 °C and 15 °C respectively, to 8.307 and 8.554 on day 13, reflecting the balance between CO₂ uptake and metabolic
265 CO₂ production over the duration of the experiment. On the last day, pCO₂ in all mesocosms ranged from 186 to 3695 µatm
266 at 10 °C and from 90 to 3480 µatm at 15 °C.

267 Nitrate (NO₃⁻) and silicic acid (Si(OH)₄) concentrations averaged 9.1 ± 0.5 µmol L⁻¹ and 13.4 ± 0.3 µmol L⁻¹ on day 0,
268 respectively (Bénard et al., 2018). The two nutrients displayed a similar temporal depletion pattern following the
269 development of the phytoplankton bloom. NO₃⁻ concentrations reached undetectable levels (<0.03 µmol L⁻¹) in all
270 mesocosms by day 5. Likewise, Si(OH)₄ fell below the detection limit (<0.1 µmol L⁻¹) between day 1 and 5 in all
271 mesocosms except for those whose pH_T was set at 7.2 and 7.6 at 10 °C (M5 and M3) and in which Si(OH)₄ depletion
272 occurred on day 9.

273 **3.2 Phytoplankton, bacterial abundance and production**

274 Chl *a* concentrations were below 1 µg L⁻¹ following the filling of the mesocosms (day -4), and had already increased to an
275 average of 5.9 ± 0.6 µg L⁻¹ on day 0 (Fig. 2a). At 10 °C, Chl *a* quickly increased to reach maximum concentrations around
276 27 ± 2 µg L⁻¹ on day 3 ± 2, and decreased progressively until the end of the experiment. Increasing the temperature by 5 °C
277 resulted in a more rapid development of the bloom and a speedier decrease of Chl *a* concentrations during the declining
278 phase of the bloom. The maximum Chl *a* concentration reached at the peak of the bloom was, however, not significantly
279 affected by the difference in temperature. We found no significant effect of the pCO₂ gradient on the mean Chl *a*
280 concentrations measured over the days 0–13, nor during the development phase and the declining phase of the bloom as
281 described in Bénard et al. (2018) (Fig. 2a–b; Table 1).

282 The free-living bacterial abundance was ~1.2 × 10⁹ cells L⁻¹ on day -4, and increased rapidly to reach 3.1 ± 0.6 × 10⁹ cells L⁻¹
283 on day 0 (Fig. 2c). This initial increase in abundance probably resulted from the release of dissolved organic matter (DOM)
284 during pumping of the seawater and filling of the mesocosms. The subsequent decrease in bacterial abundance during the
285 development phase of the bloom suggests that the initial pool of DOM was fully utilized and that freshly released DOM was
286 scarce. As expected, bacterial abundance increased during the declining phase of the bloom at 10 °C. Under warmer
287 conditions, bacterial abundance decreased earlier during the initial bloom development than was observed at 10 °C, but was
288 also marked by an earlier peak during the decline of the bloom, followed by a second, more variable peak in abundance.
289 These variations in abundances probably reflect changes in the balance between bacterial growth and loss by grazing. When
290 averaged over the experiment, we observed no effect of the treatments on the mean bacterial abundance (Fig. 2c–d; Table 1).

291 At 10 °C, bacterial production was low at the beginning of the experiment and increased gradually during the development
292 and declining phases of the bloom to reach peak values of $9.3 \pm 0.9 \mu\text{g C L}^{-1} \text{d}^{-1}$ (Fig. 2e). Bacterial production increased
293 faster at 15 °C and reached maximal production rates of $19 \pm 1 \mu\text{g C L}^{-1} \text{d}^{-1}$ on day 11. Results of the gls model show no
294 effect of the pCO_2 gradient on bacterial production, but a positive effect of warming was observable throughout the
295 experiment (Fig. 2f; Table 1).

296 **3.3 DMSP_t and DMS**

297 At in situ temperature, DMSP_t concentrations averaged $9 \pm 2 \text{ nmol L}^{-1}$ on day 0 and increased regularly in all mesocosms up
298 to day 10 before they plateaued or slightly decreased over the last 2–3 days (Fig. 3a). These results reveal that DMSP
299 accumulation persisted for several days after the bloom peaks, to reach a maximum value between days 8–13 of
300 $366 \pm 22 \text{ nmol L}^{-1}$. At 15 °C, DMSP_t concentrations similarly increased after the maximum Chl *a* concentrations were
301 reached, but increased faster than at in situ temperature. The maximum DMSP_t concentrations were $396 \pm 19 \text{ nmol L}^{-1}$ at
302 15 °C, a value that is not statistically different from the peak values measured at 10 °C (Fig 4a; Table 2). A greater loss of
303 DMSP took place in the last days of the experiment at 15 °C. By day 13, $79 \pm 3 \%$ of the peak DMSP_t concentration was lost
304 in the 15 °C mesocosms, while $19 \pm 4 \%$ of the peak DMSP_t concentration was lost at 10 °C. When averaged over the
305 duration of the experiment, the mean DMSP_t concentrations were not significantly affected by the pCO_2 gradient, the
306 temperatures or the interaction between these two factors (Fig. 3b; Table 1).

307 Over the 13 days, the DMSP_t:Chl *a* ratio averaged $11.4 \pm 0.4 \text{ nmol } (\mu\text{g Chl } a)^{-1}$ at 10 °C and was not affected by increasing
308 pCO_2 (Fig. 5; Table 1). Due to the aforementioned mismatch between the peaks in Chl *a* and DMSP_t, the average
309 DMSP_t:Chl *a* ratios were significantly higher at 15 °C, averaging $19 \pm 1 \text{ nmol } (\mu\text{g Chl } a)^{-1}$ over the experiment (Fig. 5; Table
310 1). However, we found no significant relationship between DMSP_t:Chl *a* and the pCO_2 gradient.

311 Initial DMS concentrations were below the detection limit on day 0 ($< 0.9 \text{ nmol L}^{-1}$) and slowly increased during the first 7
312 days, while most of the build-up took place after day 8 in all treatments (Fig. 3b). The net accumulation of DMS was faster
313 at 15 °C than at 10 °C, with higher daily DMS concentrations at 15 °C compared to 10 °C from day 3 until day 13. At the
314 end of the experiment, DMS concentrations averaged $21 \pm 4 \text{ nmol L}^{-1}$ at 10 °C and $74 \pm 14 \text{ nmol L}^{-1}$ at 15 °C. Over the full
315 duration of the experiment, we found significant negative effects of increasing pCO_2 on mean DMS concentrations at the two
316 temperatures tested (Fig. 3d; Table 1). At 10 °C, we measured a ~67 % reduction of mean DMS concentrations from the
317 drifter relative to the most acidified treatment (~345 ppm vs ~3200 ppm), with values decreasing from $10 \pm 2 \text{ nmol L}^{-1}$ to
318 $3.2 \pm 0.8 \text{ nmol L}^{-1}$. At 15 °C, the mean DMS concentrations decreased by roughly the same percentage (~69 %) as pCO_2
319 increased from the drifter to the most acidified treatment (~130 ppm vs ~3130 ppm). Nevertheless, the mean DMS
320 concentrations were higher at 15 °C, ranging from $34 \pm 13 \text{ nmol L}^{-1}$ to $11 \pm 3 \text{ nmol L}^{-1}$, an average increase of ~240 %
321 compared to the DMS concentrations at 10 °C (Fig. 3c; Table 1). Similarly, the peak DMS concentrations decreased linearly

322 with increasing pCO₂ at both temperatures and concentrations were always higher at 15 than at 10 °C for any given pCO₂
323 (Fig. 4b; Table 2).

324 The DMS:DMSP_t ratio exhibited the same general pattern as the DMS, i.e. low and stable values during the first 8 days, and
325 increasing values between days 8–13 (Fig. 3e). The natural logarithm of the DMS:DMSP_t ratio was not affected by the pCO₂
326 gradient at 10 °C when averaged over the 13 days experiment, but a significant decrease of the DMS:DMSP_t ratios was
327 observed with increasing pCO₂ at 15 compared to 10 °C (Fig. 3f; Table 1). Moreover, there was a significant positive
328 correlation between bacterial production and DMS concentrations, as 64 % of the variability of DMS concentrations is
329 explained by variations in bacterial production ($r^2 = 0.64$, $p < 0.001$, $n = 70$; Fig. 6).

330 **4. Discussion**

331 **4.1 General characteristics**

332 As far as we know, this study is the first full factorial mesocosm experiment where all pCO₂ treatments (pH_T from 8.0 to 7.2)
333 were replicated at two different temperatures (in situ and +5 °C), to assess the impact of ocean acidification and warming on
334 the dynamics of DMSP and DMS concentrations during a phytoplankton bloom. A diatom bloom dominated by *Skeletonema*
335 *costatum* developed in all mesocosms, regardless of the treatments. This chain-forming centric diatom is a cosmopolitan
336 species in coastal and estuarine systems and a frequent bloomer in the Lower St. Lawrence Estuary (LSLE) (Kim et al.,
337 2004; Starr et al., 2004; Annane et al., 2015). The 13 days where treatments were applied allowed us to capture the
338 development and declining phases of the bloom. The impacts of the treatments on the dynamics of the bloom during these
339 two phases are described in greater detail in Bénard et al. (2018). Briefly, the acidification had no detectable effect on the
340 development rate of the diatom bloom and on the maximum Chl *a* concentrations reached. However, increasing the water
341 temperature by 5 °C increased the growth rate of the diatoms, shortening the development phase of the bloom, from 4–7 days
342 at 10 °C to 1–4 days at 15 °C. However, these changes in the bloom timing did not alter the overall primary production
343 throughout the experiment. Hereafter, we discuss how increasing pCO₂ (lowering the pH) affected DMSP and DMS
344 concentrations and how a 5 °C increase in temperature altered the impacts of the pCO₂ gradient during the experiment.

345 **4.2. DMSP dynamics**

346 The buildup of the phytoplankton biomass during the bloom development was coupled with a rapid increase in DMSP_t
347 concentrations (Fig. 3a). Assuming that *S. costatum* was responsible for most of the DMSP production, our results indicate a
348 low sensitivity of the DMSP synthesis pathway to acidification in this species. The net accumulation of DMSP_t persisted
349 several days after the peaks in Chl *a*, indicating a decoupling between DMSP synthesis, algal growth and nitrogen
350 metabolism (Bénard et al., 2018).

351 **4.2.1 Effects of acidification on DMSP**

352 At in situ temperature, the averaged DMSP_t concentrations were not affected by the increase in pCO_2 (Fig. 3b; Table 1). The
353 lack of significant changes in the $\text{DMSP}_t:\text{Chl } a$ ratio as a function of the pCO_2 gradient also supports this conclusion (Fig. 5;
354 Table 1). This result is consistent with those of previous studies that showed a relatively weak effect of an increase in pCO_2
355 on DMSP concentrations (Vogt et al., 2008; Lee et al., 2009; Avgoustidi et al., 2012; Archer et al., 2013; Webb et al., 2015).
356 Furthermore, much like the patterns observed at 10 °C, there was no relationship between the concentrations of DMSP_t and
357 the pCO_2 gradient observable at 15 °C (Table 1).

358 **4.2.2 Effects of warming on DMSP**

359 In contrast to the absence of effects of acidification on DMSP, warming has been previously shown to affect DMSP
360 concentrations in nature. Results from shipboard incubation experiments conducted in the North Atlantic have revealed an
361 increase in particulate DMSP (DMSP_p) concentrations due to a 4 °C warming (Lee et al., 2009). During this last study, the
362 higher DMSP_p concentrations were attributed to a temperature-induced shift in community structure toward species with
363 higher cellular DMSP content. During our study, the pCO_2 and temperature treatments did not alter the structure of the
364 community (Bénard et al., 2018). Most of the DMSP synthesis was likely linked to the numerically dominant diatoms, as all
365 other algal groups identified contributed to less than 10 % of the total algal abundance (see Fig. 6 in Bénard et al., 2018).
366 Our results thus suggest that DMSP synthesis by *S. costatum* during the nitrate-replete growth phase was not significantly
367 affected by warming. Rather, it is the accelerated growth rate of *S. costatum* that promoted the concurrent accumulation of
368 biomass and DMSP_t , while the higher $\text{DMSP}_t:\text{Chl } a$ ratio observable at 15 °C may be explained by the faster degradation of
369 cells under warming. Several empty frustules were found during the last days of the experiment at 15 °C, suggesting a loss of
370 integrity of the cells and potential increase of the release of intracellular dissolved organic matter, including DMSP.
371 However, the absence of dissolved DMSP measurements prevents the verification of this suggestion. The increase in the
372 abundance of bacteria and in bacterial production (Fig. 2c, e) during that period also suggest that more dissolved organic
373 matter was produced during the decline of the bloom, as previously reported (Engel et al., 2004a, 2004b). During our
374 experiment, transparent exopolymer particles (TEP) concentrations increased during this period (Gaaloul, 2017), adding to
375 the evidence for heightened DOM production by the decaying bloom, with a potential increase in DMSP metabolism by
376 heterotrophic bacteria under warming.

377 **4.3 DMS dynamics**

378 DMS concentrations remained very low during the development phase of the bloom (day 8) and increased in the latter days
379 of the experiment. Most of the DMS accumulation in the mesocosms took place between days 8–13 and likely originated
380 from DMSP that may have been released during cell lysis (Kwint and Kramer, 1995), or upon zooplankton grazing (Cantin

381 et al., 1996). Unbalanced growth and photosynthesis of algal cells under nitrogen deficiency during that period may also be
382 responsible for a greater production and active exudation of DMSP (Stefels et al., 2000; Kettles et al., 2014).

383 4.3.1 Effects of acidification on DMS

384 At in-situ temperature, we observed a significant linear decrease in DMS concentrations (both averaged over the full
385 duration of the experiment and peak concentrations) with increasing pCO₂ (Figs. 3c, 4b; Tables 1 and 2). Few studies have
386 shown a neutral or positive effect of increasing pCO₂ on DMS concentrations, stemming from altered phytoplankton
387 taxonomy, microzooplankton grazing, or diverging bacterial activity promoting DMS production (Vogt et al., 2008; Kim et
388 al., 2010; Hopkins and Archer, 2014). However, the majority of studies have shown a decreasing trend of DMS
389 concentrations with increasing pCO₂ similar to our results (Hopkins et al., 2010; Archer et al., 2013; Park et al., 2014; Webb
390 et al., 2015, 2016). In these studies, the pCO₂-induced decreases in DMS were generally attributed to changes in the
391 microbial community speciation and structure, or to microzooplankton grazing, although decreases in bacterial DMSP-to-
392 DMS conversion or increases in DMS consumption have also been suggested (Archer et al., 2013; Hussherr et al., 2017).
393 During our study, the decrease in DMS concentrations with increasing pCO₂ cannot be directly attributed to a decrease in
394 DMSP_f since this pool was not affected by the pCO₂ gradient (Figs. 3b, 4a; Tables 1 and 2). In Park et al. (2014), the
395 increase in pCO₂ led to the reduction in the abundance of *Alexandrium* spp., an active DMSP and DMSP-lyase producer, and
396 a concomitant reduction of the associated microzooplankton grazing. As *Alexandrium* spp. was less numerous, the associated
397 attenuation of microzooplankton grazing resulted in a reduction of the mixing of DMSP and DMSP-lyase, leading to less
398 DMSP-to-DMS conversion. Given the strong contribution of *S. costatum* to the bloom, a species with no reported DMSP-
399 lyase, it can be assumed that most, if not all, of the DMS produced was driven by bacterial processes following DMSP
400 release by the diatoms. Thus, the decrease in DMS concentrations in our study could have been the result of altered bacterial
401 mediation; either through reduced bacterial production of DMS or heightened bacterial consumption of DMS. Whereas a
402 reduction in bacterial uptake of DMSP is unlikely, given that the bacterial abundance and production were unaffected by the
403 pCO₂ gradient (Table 1), the observed decrease in DMS concentrations could imply that at higher pCO₂ the bacterial yields
404 of DMS are abated. The relative proportion of DMSP consumed by bacteria and further cleaved into DMS is closely tied to
405 bacterial demand in carbon and sulfur as well as to the availability of DMSP relative to other sources of reduced sulfur in the
406 environment (Levasseur et al., 1996; Kiene et al., 2000; Pinhassi et al., 2005). The absence of a significant pCO₂ effect on
407 the concentrations of DMSP during this study may be interpreted as a pCO₂-related alteration of the microbially-mediated
408 fate of consumed DMSP. Unfortunately, in the absence of detailed ³⁵S-DMSP_d bioassays, it is impossible to confirm the
409 outcome of the DMSP metabolic pathways including the DMSP-to-DMS conversion efficiency in relation to the pCO₂
410 gradient. A few studies (Grossart et al., 2006; Engel et al., 2014; Webb et al., 2015;) have reported enhanced bacterial
411 abundance and production at high pCO₂, especially for attached bacteria as opposed to free-living (Grossart et al., 2006).
412 However, regardless of the temperature treatment, neither the abundance nor the activity of bacteria seemed to be
413 significantly impacted by pCO₂ in this study. A pCO₂-induced increase in bacterial DMS turnover could also explain the

414 decrease in DMS concentrations, but several studies suggest that bacterial DMS consumption in natural systems is often
415 tightly coupled to DMS production itself (Simó, 2001, 2004). Furthermore, while one laboratory study reported that non-
416 limiting supplies of DMS may be used as a substrate by several members of Bacteroidetes (Green et al., 2011), another study
417 showed that only a subset of the natural microbial population may turnover naturally-occurring levels of DMS (Vila-Costa et
418 al., 2006b). Nevertheless, the sensitivity of these DMS-consuming bacteria to decreasing pH remains unknown. Likewise,
419 whereas we cannot exclude a potential impact of pCO₂ on DMS turnover via bacterioplankton, it is plausible that the pCO₂
420 gradient may have affected a widespread physiological pathway among bacteria, specifically, the metabolic breakdown of
421 DMSP.

422 **4.3.2 Effects of warming on DMS**

423 A warming by 5 °C increased DMS concentrations at all pCO₂ tested, resulting in an offset of the negative pCO₂ impact
424 when compared to the in situ temperature. This result differs from the observation of Kim et al. (2010) and Park et al. (2014)
425 in two ways. First, our results show an increase in DMS concentrations in the warmer treatment while the two previous
426 studies reported a decrease. Second, our results confirm that a temperature effect may be measured over a large range of
427 pCO₂. It is noteworthy that the increase in DMS concentrations at the two temperatures tested varied from 110 % at pH 8.0
428 up to 370 % at pH 7.4. This highlights the scaling of the temperature effect over an extensive range of pCO₂ and the
429 importance of simultaneously studying the impact of these two factors on DMS production. As observed at 10 °C, both the
430 average and the peak DMS concentrations decreased linearly as pCO₂ increased in the warm treatment (Figs. 3d, 4b; Tables
431 1 and 2). Nevertheless, the pCO₂-induced decrease in DMS concentrations at 15 °C cannot be directly attributed to a
432 decrease in DMSP_t concentrations given that an increase in pCO₂ had no discernable effect on DMSP_t concentrations. In
433 contrast to our observations at the in situ temperature, where DMSP_t continued to increase until day 12, DMSP_t
434 concentrations at 15 °C typically decreased from day 8 onward (Fig. 3a). This loss in DMSP_t suggests that microbial
435 consumption of DMSP exceeded DMSP algal synthesis. In light of the dominance of *S. costatum*, a phytoplankton taxon not
436 known to exhibit DMSP-lyase, the bulk of microbial DMSP mediation was likely associated with heterotrophic bacteria. In
437 support of this hypothesis, the bacterial production was ~2 times higher at 15 than at 10 °C between days 8–13
438 ($19 \pm 1 \mu\text{g C L}^{-1} \text{d}^{-1}$ vs $9.3 \pm 0.9 \mu\text{g C L}^{-1} \text{d}^{-1}$) (Fig. 2), and we observed a significant correlation between the quantity of
439 DMSP_t lost between the day of the maximum DMSP_t concentrations and day 13, and the quantity of DMS produced during
440 the same period (coefficient of determination, $r^2 = 0.60$, $p < 0.01$, $n = 11$). Assuming that all the DMSP_t lost was transformed
441 into DMS by bacteria, we calculated that DMS yields could have varied by 0.5 to 32 % across the pCO₂ gradient (mean =
442 13 ± 11 %). These very rough estimates of DMS yields are likely at the lower end since measured DMS concentrations also
443 reflect losses of DMS through photo-oxidation and bacterial consumption. Nevertheless, we cannot exclude the possibility of
444 some passive uptake of DMSP by the picocyanobacterial population in the mesocosms, although this pathway is not
445 considered to be significant in natural systems (Malmstrom et al., 2005; Vila-Costa et al., 2006a) and does not lead to the
446 production of DMS. Moreover, our estimates do not account for the possible DMSP assimilation by grazers, reducing the

447 DMSP_d available for bacteria, and would lead to an increase in DMS yields. Our ‘minimum community’ DMS yield
448 estimates agree with an expected range of microbial DMS yields in natural environments, from 2 % to 45 % (see review
449 table in Lizotte et al., 2017). These gross but realistic estimates of heterotrophic bacterial DMSP-to-DMS conversions could
450 explain the bulk of the DMS present in our study, a hypothesis also supported by the strong positive correlation ($r^2 = 0.64$,
451 $p < 0.001$, $n = 70$; Fig. 6) between overall DMS concentrations and bacterial production. Combined, these findings reinforce
452 the idea that bacterial metabolism, rather than bacterial stocks, may significantly affect the fate of DMSP (Malmstrom et al.,
453 2004a, 2004b, 2005; Vila et al., 2004; Vila-Costa et al., 2007; Royer et al., 2010; Lizotte et al., 2017). Consequently, drivers
454 of environmental change, such as temperature and pH, could alter bacterial activity and strongly impact the concentrations of
455 DMS by controlling the rates of production and loss of DMS by bacteria. Specific measurements of bacterial DMSP uptake
456 and DMS yields using ³⁵S-DMSP_d should be conducted to assess the impacts of pCO₂ and temperature on the microbial fate
457 of DMSP.

458 **4.4 Limitations**

459 During our study, the pCO₂ changes were applied abruptly, over a day, from in situ values to pCO₂ levels exceeding the most
460 pessimistic pCO₂ scenarios for the end of the century. Compared to our manipulation, ocean acidification will proceed at a
461 much slower rate, potentially allowing species to adapt and evolve to these changing conditions (Stillman and Paganini,
462 2015; Schlüter et al., 2016). However, in the LSLE, the upwelling of low oxygenated waters can rapidly reduce the pH_T to
463 ~7.62, or even lower with contributions of low pH_T (7.12) freshwaters from the Saguenay River during the spring freshet
464 (Mucci et al., 2017). Thus, the swift and extensive pCO₂ range deployed in our experiment may seem improbable for the
465 open ocean on the short term, but may not be inconceivable for this coastal region. However, the warming of 5 °C used in
466 this mesocosm study possibly exceeds the upper limit of temperature increase for the end of the century in this region. In the
467 adjacent Gulf of St. Lawrence (GSL), surface waters temperature (SST) correlates strongly with air temperature, allowing
468 the estimation of past SST. This relationship showed that SST has increased in the GSL by 0.9 °C per century since 1873
469 (Galbraith et al., 2012), although additional positive anomalies of 0.25–0.75 °C per decade have been shown between 1985
470 and 2013 (Galbraith et al., 2016). In the LSLE, the highest temperatures occur at the end of summer / early fall, and
471 gradually dissipate by heating the subjacent cold intermediate layer through vertical mixing (Cyr et al., 2011). The extent of
472 the projected warming in the LSLE is recondite, but will likely result from the multifaceted interactions between heat
473 transfer from the air and physical factors controlling the water masses.

474 The results from our study could also be influenced by the absence of macrograzers in the mesocosms. An additional grazing
475 pressure could limit the growth of the blooming species, reducing the amount of DMSP produced or could increase the
476 release of DMSP_d through sloppy feeding after the initial bloom (Lee et al., 2003). It is unclear how an increase in grazing
477 pressure would have impacted the concentrations of DMS in our experiment. On the one hand, increased predation could
478 have limited the net accumulation of DMSP_p, with a possible reduction in DMS production. On the other hand, increased
479 grazing could have favoured the release of DMSP_p as DMSP_d, thus increasing the availability of this substrate for microbial

480 uptake, mediation and possible conversion into DMS. Despite the absence of reported changes in community composition in
481 our study, many OA mesocosm experiments have described changes in DMS concentrations associated with shifts in
482 community structure in the past (Vogt et al., 2008; Hopkins et al., 2010; Kim et al., 2010, Park et al., 2014, Webb et al.,
483 2015). Nonetheless, our results align with those of other OA studies (Archer et al., 2013; Hussherr et al., 2017), suggesting
484 that the mediation of heterotrophic bacteria plays a major role in DMS cycling in the absence of reported phytoplanktonic
485 DMSP-lyase, such as in a diatom dominated bloom in the LSLE.

486 **5. Conclusions**

487 The objective of this study was to quantify the combined impact of increases in pCO₂ and temperature on the dynamics of
488 DMS during a fall diatom bloom in the St. Lawrence Estuary. Our mesocosm experiment allowed us to capture the
489 development and declining phases of a bloom strongly dominated by the diatom *Skeletonema costatum* and the related
490 changes in bacterial abundance and production. As expected, warming accelerated the development of the bloom, but also its
491 decline. Both DMSP_i and DMS concentrations increased during the development phase of the bloom, but their peak
492 concentrations were reached as the bloom was declining. Increasing pCO₂ had no discernable effect on the total amount of
493 DMSP_i produced at both temperatures tested. In contrast, increasing the pCO₂ to the value forecasted for the end of this
494 century resulted in a linear decrease in DMS concentrations by 33 % and by as much as 69 % over the full pCO₂ gradient
495 tested. These results are consistent with previous reports that acidification has a greater impact on the processes that control
496 the conversion of DMSP to DMS than on the production of DMSP itself. The pCO₂-induced decrease in DMS
497 concentrations observed in this study adds to the bulk of previous studies reporting a similar trend. In diatom dominated
498 systems, such as the one under study in this experiment, heterotrophic processes underlying DMS production seem to be
499 most sensitive to modifications in pCO₂. Whereas predatory grazing and its associated impacts on DMS production cannot
500 be ruled out entirely, the decreases in DMS concentrations in response to heightened pCO₂ are likely related to reductions in
501 bacterial-mediated DMS production, a hypothesis partly supported by the significant positive correlations found between
502 DMS concentrations and bacterial production. Whereas the DMS concentrations decreased significantly with increasing
503 pCO₂ at both 10 °C and 15 °C, warming the mesocosms by 5 °C translated into a positive offset in concentrations of DMS
504 over the whole range of pCO₂ tested. Higher DMSP release and increased bacterial productivity in the warm treatment
505 partially explain the stimulating effect of temperature on DMS net production. Overall, results from this full factorial
506 mesocosm experiment suggest that warming could mitigate the expected reduction in DMS production due to ocean
507 acidification, even increasing the net DMS production with the potential to curtail radiative forcing. Further studies should
508 focus on the relationship between bacterial conversion of DMSP to DMS and pCO₂, to mechanistically verify the suggested
509 cause of the DMS reduction observed in this experiment. Moreover, an extended range of temperature should also be
510 considered for future multiple stressors experiment as warming had, more often than not, a stronger effect on the community
511 than acidification.

512 *Data availability.* The data have been submitted to be freely accessible via Pangaea or can be obtained by contacting the
513 author (robin.benard.1@ulaval.ca).

514 *Author contributions.* R. B nard was responsible for the experimental design elaboration, data sampling and processing, and
515 the writing of this article. Several co-authors supplied specific data included in this article, and all co-authors contributed to
516 this final version of the article.

517 *Competing interests.* The authors declare that they have no conflict of interest.

518 **Acknowledgements**

519 The authors wish to thank the Station Aquicole-ISMER, particularly Nathalie Morin and her staff, for their support during
520 the mesocosm experiment. We also wish to acknowledge Gilles Desmeules, Bruno Cayouette, Sylvain Blondeau, Claire Lix,
521 Rachel Hussherr, Liliane St-Amand, Marjolaine Blais, Armelle Galine Simo Matchim and Marie-Am lie Blais for their
522 precious help over the duration of the experiment. This study was funded by a Team grant from the Fonds de recherche du
523 Qu bec – Nature et technologies (FRQNT- quipe-165335), the Canada Foundation for Innovation, the Canada Research
524 Chair on Ocean Biogeochemistry and Climate, Fisheries and Oceans Canada, and by the Major International Joint Research
525 Project of the National Natural Science Foundation of China (Grant no. 41320104008). This is a contribution to the research
526 program of Qu bec-Oc an.

527 **References**

528 Andreae, M. O.: Ocean-atmosphere interactions in the global biogeochemical sulfur cycle, *Mar. Chem.*, 30, 1–3, 1990.
529 Andreae, M.O. and Crutzen, P. J.: Atmospheric aerosols: biogeochemical sources and role in atmospheric chemistry,
530 *Science*, 276(5315), 1052–1058, doi:10.1126/science.276.5315.1052, 1997.
531 Annane, S., St-Amand, L., Starr, M., Pelletier, E., and Ferreyra, G. A.: Contribution of transparent exopolymeric particles
532 (TEP) to estuarine particulate organic carbon pool, *Mar. Ecol. Prog. Ser.*, 529, 17–34, doi:10.3354/meps11294, 2015.
533 Avgoustidi, V., Nightingale, P. D., Joint, I., Steinke, M., Turner, S. M., Hopkins, F. E., and Liss, P. S.: Decreased marine
534 dimethyl sulfide production under elevated CO₂ levels in mesocosm and in vitro studies, *Environ. Chem.*, 9(4), 399,
535 doi:10.1071/EN11125, 2012.
536 Barnard, W.R., Andreae, M.O., Watkins, W.E., Bingemer, H., and Georgii, H.W.: The flux of dimethylsulfide from the
537 oceans to the atmosphere. *J. Geophys. Res.*, 87(C11), 8787–8793, 1982.
538 Bates, T. S., Lamb, B. K., Guenther, A., Dignon, J., and Stoiber, R. E.: Sulfur emissions to the atmosphere from natural
539 sources, *J. Atmos. Chem.*, 14(1–4), 315–337, doi:10.1007/BF00115242, 1992.

540 Bell, R. T.: Estimating production of heterotrophic bacterioplankton via incorporation of tritiated thymidine, in: Handbook
541 of methods in aquatic microbial ecology, Eds: Kemp, P. F., Sherr, B. F., Sherr, E. B., and Cole, J., Lewis Publisher, Boca
542 Raton, 495–503, 1993.

543 Belzile, C., Brugel, S., Nozais, C., Gratton, Y. and Demers, S.: Variations of the abundance and nucleic acid content of
544 heterotrophic bacteria in Beaufort Shelf waters during winter and spring, *J. Mar. Syst.*, 74(3–4), 946–956,
545 doi:10.1016/j.jmarsys.2007.12.010, 2008.

546 B nard, R., Levasseur, M., Scarratt, M. G., Blais, M.-A., Mucci, A., Ferreyra, G., Starr, M., Gosselin, M., Tremblay, J.- .,
547 and Lizotte, M.: Experimental assessment of the sensitivity of an estuarine phytoplankton fall bloom to acidification and
548 warming, *Biogeosciences*, 15, 4883–4904, <https://doi.org/10.5194/bg-15-4883-2018>, 2018.

549 Boyd, P. W., Lennartz, S. T., Glover, D. M. and Doney, S. C.: Biological ramifications of climate-change-mediated oceanic
550 multi-stressors, *Nat. Clim. Chang.*, 5(1), 71–79, doi:10.1038/nclimate2441, 2015.

551 Boyd, P. W., Collins, S., Dupont, S., Fabricius, K., Gattuso, J.-P., Havenhand, J., Hutchins, D. A., Riebesell, U., Rintoul, M.
552 S., Vichi, M., Biswas, H., Ciotti, A., Gao, K., Gehlen, M., Hurd, C. L., Kurihara, H., McGraw, C. M., Navarro, J. M.,
553 Nilsson, G. E., Passow, U. and P rtner, H.-O.: Experimental strategies to assess the biological ramifications of multiple
554 drivers of global ocean change-A review, *Glob. Chang. Biol.*, 24(6), 2239–2261, doi:10.1111/gcb.14102, 2018.

555 Brimblecombe, P., and Shooter, D.: Photo-oxidation of dimethylsulphide in aqueous solution, *Mar. Chem.*, 19, 343–353,
556 1986.

557 Byrne, R. H.: Standardization of Standard Buffers by Visible Spectrometry, *Anal. Chem*, 59, 1479–1481,
558 doi:10.1021/ac00137a025, 1987.

559 Caldeira, K., and Wickett, M. E.: Ocean model predictions of chemistry changes from carbon dioxide emissions to the
560 atmosphere and ocean, *J. Geophys. Res.*, 110(C9), 1–12, doi:10.1029/2004JC002671, 2005.

561 Cai, W. J., and Wang, Y.: The chemistry, fluxes, and sources of carbon dioxide in the estuarine waters of the Satilla and
562 Altamaha Rivers, Georgia, *Limnol. Oceanogr.*, 43(4), 657–668, doi:10.4319/lo.1998.43.4.0657, 1998.

563 Cantin, G., Levasseur, M., Gosselin, M., Michaud, S.: Role of zooplankton in the mesoscale distribution of surface
564 dimethylsulfide concentrations in the Gulf of St. Lawrence, Canada, *Mar. Ecol. Prog. Ser.*, 141, 103–117, 1996.

565 Cantoni, G. L. and Anderson, D. Enzymatic cleavage of dimethylpropiothetin by *Polysiphonia Lanosa*, *J. Bio. Chem.*, 222,
566 171–177, 1956.

567 Carslaw, K. S., Boucher, O., Spracklen, D. V., Mann, G. W., Rae, J. G. L., Woodward, S., and Kulmala, M.: A review of
568 natural aerosol interactions and feedbacks within the Earth system, *Atmos. Chem. Phys.*, 10, 1701–1737, doi:10.5194/acp-
569 10-1701- 2010, 2010.

570 Charlson, R., Lovelock, J., Andreae, M., and Warren, S.: Oceanic phytoplankton, atmospheric sulphur, cloud albedo and
571 climate, *Nature*, 326, 656–661, 1987.

572 Clayton, T. D., and Byrne, R. H.: Spectrophotometric seawater pH measurements: total hydrogen ion concentration scale
573 calibration of m-cresol purple and at-sea results, *Deep. Res. Part I*, 40(10), 2115–2129, doi:10.1016/0967-0637(93)90048-8,
574 1993.

575 Cyr, F., Bourgault, D., and Galbraith, P. S.: Interior versus boundary mixing of a cold intermediate layer, *J. Geophys. Res.*
576 *Ocean.*, 116(12), 1–12, doi:10.1029/2011JC007359, 2011.

577 Dacey, J. W. H., and Wakeham, S. G.: Oceanic dimethylsulfide: production during zooplankton grazing, *Science*, 233,
578 1314–1316, 1986.

579 Dickson, A. G.: Standard potential of the reaction: $\text{AgCl(s)} + 1\ 2\text{H}_2(\text{g}) = \text{Ag(s)} + \text{HCl(aq)}$ and the standard acidity constant
580 of the ion HSO_4^- in synthetic sea water from 273.15 to 318.15 K, *J. Chem. Thermodyn.*, 22(2), 113–127, doi:10.1016/0021-
581 9614(90)90074-Z, 1990.

582 Doney, S. C., Fabry, V. J., Feely, R. A., and Kleypas, J. A.: Ocean acidification: The other CO₂ problem, *Ann. Rev. Mar.*
583 *Sci.*, 1(1), 169–192, doi:10.1146/annurev.marine.010908.163834, 2009.

584 Engel, A., Delille, B., Jacquet, S., Riebesell, U., Rochelle-Newall, E., Terbrüggen, A., and Zondervan, I.: Transparent
585 exopolymer particles and dissolved organic carbon production by *Emiliania huxleyi* exposed to different CO₂ concentrations:
586 A mesocosm experiment, *Aquat. Microb. Ecol.*, 34(1), 93–104, doi:10.3354/ame034093, 2004a.

587 Engel, A., Thoms, S., Riebesell, U., Rochelle-Newall, E., and Zondervan, I.: Polysaccharide aggregation as a potential sink
588 of marine dissolved organic carbon, *Nature*, 428(6986), 929–932, doi:10.1038/nature02453, 2004b.

589 Engel, A., Piontek, J., Grossart, H.-P., Riebesell, U., Schulz, K. G., and Sperling, M.: Impact of CO₂ enrichment on organic
590 matter dynamics during nutrient induced coastal phytoplankton blooms, *J. Plankton Res.*, 36(3), 641–657,
591 doi:10.1093/plankt/fbt125, 2014.

592 Feely, R. A., Doney, S. C., and Cooley, S. R.: Ocean Acidification: Present Conditions and Future Changes in a High-CO₂
593 World, *Oceanography*, 22(4), 36–47, doi:DOI 10.5670/oceanog.2009.95, 2009.

594 Fuhrman, J. A., and Azam, F.: Bacterioplankton secondary production estimates for coastal waters of British Columbia,
595 Antarctica, and California, *Appl. Environ. Microbiol.*, 39(6), 1085–1095, 1980.

596 Fuhrman, J. A., and Azam, F.: Thymidine incorporation as a measure of heterotrophic bacterioplankton production in marine
597 surface waters: Evaluation and field results, *Mar. Biol.*, 66(2), 109–120, doi:10.1007/BF00397184, 1982.

598 Gaaloul, H.: Effets du changement global sur les particules exopolymériques transparentes au sein de l'estuaire maritime du
599 Saint-Laurent, M.Sc. thesis, Université du Québec à Rimouski, Canada, 133 pp., 2017.

600 Galbraith, P. S., Chassé, J., Gilbert, D., Larouche, P., Brickman, D., Pettigrew, B., Devine, L., Gosselin, A., Pettipas, R. G.,
601 and Lafleur, C.: Physical Oceanographic Conditions in the Gulf of St. Lawrence in 2011, *DFO Can. Sci. Advis. Sec. Res.*
602 *Doc.*, 2012/023, iii + 85 pp, 2012.

603 Galbraith, P. S., Chassé, J., Caverhill, C., Nicot, P., Gilbert, D., Pettigrew, B., Lefaiivre, D., Brickman, D., Devine, L., and
604 Lafleur, C.: Physical Oceanographic Conditions in the Gulf of St. Lawrence in 2015, *DFO Can. Sci. Advis. Sec. Res. Doc.*,
605 2016/056, v + 90 pp, 2016.

606 Gattuso, J.-P., Magnan, A., Bille, R., Cheung, W. W. L., Howes, E. L., Joos, F., Allemand, D., Bopp, L., Cooley, S. R.,
607 Eakin, C. M., Hoegh-Guldberg, O., Kelly, R. P., Portner, H.-O., Rogers, a. D., Baxter, J. M., Laffoley, D., Osborn, D.,
608 Rankovic, A., Rochette, J., Sumaila, U. R., Treyer, S., and Turley, C.: Contrasting futures for ocean and society from
609 different anthropogenic CO₂ emissions scenarios, *Science*, 349(6243), doi:10.1126/science.aac4722, 2015.

610 Green, D.H., Shenoy, D. M., Hart, M. C., and Hatton, A. D.: Coupling of dimethylsulfide oxidation to biomass production
611 by a marine Flavobacterium, *Appl. Environ. Microbiol.*, 77(9), 3137–3140, doi:10.1128/AEM.02675-10, 2011.

612 Grossart, H.-P., Allgaier, M., Passow, U., and Riebesell, U.: Testing the effect of CO₂ concentration on the dynamics of
613 marine heterotrophic bacterioplankton, *Limnol. Oceanogr.*, 51(1), 1–11, doi:10.4319/lo.2006.51.1.0001, 2006.

614 Gunderson, A. R., Armstrong, E. J., and Stillman, J. H.: Multiple Stressors in a Changing World: The Need for an Improved
615 Perspective on Physiological Responses to the Dynamic Marine Environment, *Ann. Rev. Mar. Sci.*, 8(1), 357–378,
616 doi:10.1146/annurev-marine-122414-033953, 2016.

617 Hansen, H. P., and Koroleff, F.: Determination of nutrients, in: *Methods of Seawater Analysis*, 3, Eds: Grasshoff K.,
618 Kremling, K., and Ehrhardt, M., Wiley-VCH Verlag GmbH, Weinheim, Germany, 159–228,
619 doi:10.1002/9783527613984.ch10, 2007.

620 Hatton, A. D., Darroch, L., and Malin, G.: The role of dimethylsulphoxide in the marine biogeochemical cycle of
621 dimethylsulphide, *Oceanogr. Mar. Biol. An Annu. Rev.*, 42, 29–56, 2004.

622 Hopkins, F. E., and Archer, S. D.: Consistent increase in dimethyl sulfide (DMS) in response to high CO₂ in five shipboard
623 bioassays from contrasting NW European waters, *Biogeosciences*, 11(18), 4925–4940, doi:10.5194/bg-11-4925-2014, 2014.

624 Hopkins, F. E., Turner, S. M., Nightingale, P. D., Steinke, M., Bakker, D., and Liss, P. S.: Ocean acidification and marine
625 trace gas emissions, *Proc. Natl. Acad. Sci.*, 107(2), 760–765, doi:10.1073/pnas.0907163107, 2010.

626 Hussherr, R., Levasseur, M., Lizotte, M., Tremblay, J. É., Mol, J., Thomas, H., Gosselin, M., Starr, M., Miller, L. A.,
627 Jarníková, T., Schuback, N., and Mucci, A.: Impact of ocean acidification on Arctic phytoplankton blooms and dimethyl
628 sulfide concentration under simulated ice-free and under-ice conditions, *Biogeosciences*, 14(9), 2407–2427, doi:10.5194/bg-
629 14-2407-2017, 2017.

630 IPCC: Working Group I Contribution to the Fifth Assessment Report Climate Change 2013: The Physical Science Basis,
631 Intergov. Panel Clim. Chang., 1535, doi:10.1017/CBO9781107415324., 2013.

632 Iverson, R. L., Nearhoof, F. L. and Andreae, M. O.: Production of dimethylsulfonium propionate and dimethylsulfide by
633 phytoplankton in estuarine and coastal waters, *Limnol. Oceanogr.*, 34(1), 53–67, doi:10.4319/lo.1989.34.1.0053, 1989.

634 Karsten, U., Kück, K., Vogt, C., and Kirst, G. O.: Dimethylsulfoniopropionate production in phototrophic organisms and its
635 physiological functions as a cryoprotectant, in: *Biological and environmental chemistry of DMSP and related sulfonium*
636 *compounds*, Eds: Kiene, R. P., Visscher, P. T., Keller, M. D., and Kirst, G. O., Springer US, Boston, MA, 143–153,
637 doi:10.1007/978-1-4613-0377-0, 1996.

638 Keller, M. D.: Dimethyl sulfide production and marine phytoplankton: the importance of species composition and cell size,
639 *Biol. Oceanogr.*, 6(5–6), 375–382, doi:10.1080/01965581.1988.10749540, 1989.

640 Kettle, A. J., Andreae, M. O., Amouroux, D., Andreae, T. W., Bates, T. S., Berresheim, H., Bingemer, H., Boniforti, R.,
641 Curran, M. A. J., diTullio, G. R., Helas, G., Jones, G. B., Keller, I. M. D., Kiene, R. P., Leck, C., Levasseur, M., Maspero,
642 M., Matrai, P., McTaggart, A. R., Mihalopoulos, N., Nguyen, B. C., Novo, A., Putaud, J. P., Rapsomanikis, S., Roberts, G.,
643 Schebeske, G.; Sharma, S., Simó, R., Staubes, R., Turner, S., and Uher, G.: A global database of sea surface dimethylsulfide
644 (DMS) measurements and a procedure to predict sea surface DMS as a function of latitude, longitude, and month, *Global*
645 *Biogeochem. Cycles*, 13, 399-444, 1999.

646 Kettles, N. L., Kopriva, S., and Malin, G.: Insights into the regulation of DMSP synthesis in the diatom *Thalassiosira*
647 *pseudonana* through APR activity, proteomics and gene expression analyses on cells acclimating to changes in salinity, light
648 and nitrogen, *PLoS One*, 9(4), doi:10.1371/journal.pone.0094795, 2014.

649 Kiene, R. P., Linn, L. J.: Distribution and turnover of dissolved DMSP and its relationship with bacterial production and
650 dimethylsulfide in the Gulf of Mexico, *Limnol. Oceanogr.*, 45, 849–861, 2000.

651 Kiene, R. P., and Service, S. K.: Decomposition of dissolved DMSP and DMS in estuarine waters: dependence on
652 temperature and substrate concentration, *Mar. Ecol. Prog. Ser.*, 76, 1–11, 1991.

653 Kiene, R. P., Linn, L. J., Gonzalez, J., Moran, M. A., and Bruton, J. A.: Dimethylsulfoniopropionate and methanethiol are
654 important precursors of methionine and protein-sulfur in marine bacterioplankton, *Appl Environ. Microbiol.*, 65, 4549–4558,
655 1999.

656 Kiene, R. P., Linn, L. J., and Bruton, J. A. New and important roles for DMSP in marine microbial communities, *J. Sea.*
657 *Res.*, 43, 209–224, 2000.

658 Kim, K. Y., Garbary, D. J., and McLachlan, J. L.: Phytoplankton dynamics in Pomquet Harbour, Nova Scotia: a lagoon in the
659 southern Gulf of St Lawrence, *Phycologia*, 43(3), 311–328, 2004.

660 Kim, J. M., Lee, K., Yang, E. J., Shin, K., Noh, J. H., Park, K. T., Hyun, B., Jeong, H. J., Kim, J. H., Kim, K. Y., Kim, M.,
661 Kim, H. C., Jang, P. G. and Jang, M. C.: Enhanced production of oceanic dimethylsulfide resulting from CO₂-induced
662 grazing activity in a high CO₂ world, *Environ. Sci. Technol.*, 44(21), 8140–8143, doi:10.1021/es102028k, 2010.

663 Kirst, G. O., Thiel, C., Wolff, H., Nothnagel, J., Wanzek M., and Ulmke, R.: Dimethylsulfoniopropionate (DMSP) in ice-
664 algae and its possible biological role, *Mar. Chem.*, 35, 381–388, 1991.

665 Kwint, R. L., and Kramer, K. J.: Dimethylsulphide production by plankton communities, *Mar. Ecol. Prog. Ser.*, 121(1–3),
666 227–238, doi:10.3354/meps121227, 1995.

667 Hill, R. W., White, B. A., Cottrell, M. T., Dacey, J. W. H.: Virus-mediated total release of dimethylsulfoniopropionate from
668 marine phytoplankton: a potential climate process, *Aquat. Microb. Ecol.*, 14, 1–6, 1998.

669 Lana, A., Bell, T. G., Simó, R., Vallina, S. M., Ballabrera-Poy, J., Kettle, a. J., Dachs, J., Bopp, L., Saltzman, E. S., Stefels,
670 J., Johnson, J. E., and Liss, P. S.: An updated climatology of surface dimethylsulfide concentrations and emission fluxes in
671 the global ocean, *Global Biogeochem. Cycles*, 25(1), 1–17, doi:10.1029/2010GB003850, 2011.

672 Laroche, D., Vézina, A. F., Levasseur, M., Gosselin, M., Stefels, J., Keller, M. D., Matrai, P. A., and Kwint, R. L. J.: DMSP
673 synthesis and exudation in phytoplankton: A modeling approach, *Mar. Ecol. Prog. Ser.*, 180(May), 37–49,
674 doi:10.3354/meps180037, 1999.

675 Lee, P. A., Saunders, P. A., De Mora, S. J., Deibel, D. and Levasseur, M.: Influence of copepod grazing on concentrations of
676 dissolved dimethylsulfoxide and related sulfur compounds in the North Water, Northern Baffin Bay, *Mar. Ecol. Prog. Ser.*,
677 255, 235–248, doi:10.3354/meps255235, 2003.

678 Lee, P. A., Rudisill, J. R., Neeley, A. R., Maucher, J. M., Hutchins, D. A., Feng, Y., Hare, C. E., Leblanc, K., Rose, J. M.,
679 Wilhelm, S. W., Rowe, J. M., and Giacomo, R.: Effects of increased pCO₂ and temperature on the North Atlantic spring
680 bloom. III. Dimethylsulfoniopropionate, *Mar. Ecol. Prog. Ser.*, 388, 41–49, doi:10.3354/meps08135, 2009.

681 Le Quéré, C., Andres, R. J., Boden, T., Conway, T., Houghton, R. A., House, J. I., Marland, G., Peters, G. P., Van Der Werf,
682 G. R., Ahlström, A., Andrew, R. M., Bopp, L., Canadell, J. G., Ciais, P., Doney, S. C., Enright, C., Friedlingstein, P.,
683 Huntingford, C., Jain, A. K., Jourdain, C., Kato, E., Keeling, R. F., Klein Goldewijk, K., Levis, S., Levy, P., Lomas, M.,
684 Poulter, B., Raupach, M. R., Schwinger, J., Sitch, S., Stocker, B. D., Viovy, N., Zaehle, S., and Zeng, N.: The global carbon
685 budget 1959-2011, *Earth Syst. Sci. Data*, 5(1), 165–185, doi:10.5194/essd-5-165-2013, 2013.

686 Le Quéré, C., Moriarty, R., andrew, R. M., Canadell, J. G., Sitch, S., Korsbakken, J. I., Friedlingstein, P., Peters, G. P.,
687 andres, R. J., Boden, T. A., Houghton, R. A., House, J. I., Keeling, R. F., Tans, P., Arneeth, A., Bakker, D. C. E., Barbero, L.,
688 Bopp, L., Chang, J., Chevallier, F., Chini, L. P., Ciais, P., Fader, M., Feely, R. A., Gkritzalis, T., Harris, I., Hauck, J., Ilyina,
689 T., Jain, A. K., Kato, E., Kitidis, V., Klein Goldewijk, K., Koven, C., Landschützer, P., Lauvset, S. K., Lefèvre, N., Lenton,
690 A., Lima, I. D., Metzl, N., Millero, F., Munro, D. R., Murata, A., S. Nabel, J. E. M., Nakaoka, S., Nojiri, Y., O'Brien, K.,
691 Olsen, A., Ono, T., Pérez, F. F., Pfeil, B., Pierrot, D., Poulter, B., Rehder, G., Rödenbeck, C., Saito, S., Schuster, U.,
692 Schwinger, J., Séférian, R., Steinhoff, T., Stocker, B. D., Sutton, A. J., Takahashi, T., Tilbrook, B., Van Der Laan-Luijckx, I.
693 T., Van Der Werf, G. R., Van Heuven, S., Vandemark, D., Viovy, N., Wiltshire, A., Zaehle, S., and Zeng, N.: Global Carbon
694 Budget 2015, *Earth Syst. Sci. Data*, 7(2), 349–396, doi:10.5194/essd-7-349-2015, 2015.

695 Levasseur, M., Michaud, S., Egge, J., Cantin, G., Nejstgaard, J. C., Sanders, R., Fernandez, E., Solberg, P. T., Heimdal, B.,
696 and Gosselin, M.: Production of DMSP and DMS during a mesocosm study of an *Emiliania huxleyi* bloom: Influence of
697 bacteria and *Calanus finmarchicus* grazing, *Mar. Biol.*, 126(4), 609–618, doi:10.1007/BF00351328, 1996.

698 Liss, P. S. and Lovelock, J. E.: Climate change: The effect of DMS emissions, *Environ. Chem.*, 4(6), 377–378,
699 doi:10.1071/EN07072, 2007.

700 Lizotte, M., Levasseur, M., Michaud, S., Scarratt, M. G., Merzouk, A., Gosselin, M., Pommier, J., Rivkin, R. B., and Kiene,
701 R. P.: Macroscale patterns of the biological cycling of dimethylsulfoniopropionate (DMSP) and dimethylsulfide (DMS) in
702 the Northwest Atlantic, *Biogeochemistry*, 110(1–3), 183–200, doi:10.1007/s10533-011-9698-4, 2012.

703 Lizotte, M., Levasseur, M., Law, C. S., Walker, C. F., Safi, K. A., Marriner, A. and Kiene, R. P.:
704 Dimethylsulfoniopropionate (DMSP) and dimethyl sulfide (DMS) cycling across contrasting biological hotspots of the New
705 Zealand subtropical front, *Ocean Sci.*, 13(6), 961–982, doi:10.5194/os-13-961-2017, 2017.

706 Lovelock, J. E., Maggs, R. J., and Rasmussen R. A.: Atmospheric dimethyl sulfide and natural sulfur cycle, *Nature*,
707 237(5356), 452-453, 1972.

708 Malin, G., and Kirst, G. O.: Algal production of dimethyl sulfide and its atmospheric role, *J. Phycol.*, 33, 889-896, 1997.

709 Malin, G., Wilson, W. H., Bratbak, G., Liss, P. S., and Mann, N. H.: Elevated production of dimethylsulfide resulting from
710 viral infection of cultures of *Phaeocystis pouchetii*, *Limnol. Oceanogr.*, 43(6), 1389–1393, doi:10.4319/lo.1998.43.6.1389,
711 1998.

712 Malmstrom, R. R., Kiene, R. P., Cottrell, M. T., and Kirchman, D. L.: Contribution of SAR11 bacteria to dissolved
713 dimethylsulfoniopropionate and amino acid uptake in the north Atlantic Ocean, *Appl. Environ. Microbiol.*, 70(7), 4129–
714 4135, doi:10.1128/AEM.70.7.4129, 2004a.

715 Malmstrom, R. R., Kiene, R. P., and Kirchman, D. L.: Identification and enumeration of bacteria assimilating
716 dimethylsulfoniopropionate (DMSP) in the North Atlantic and Gulf of Mexico, *Limnol. Oceanogr.*, 49, 597–606, doi:
717 10.4319/lo.2004.49.2.0597, 2004b.

718 Malmstrom, R. R., Kiene, R. P., Vila, M., and Kirchman, D. L.: Dimethylsulfoniopropionate (DMSP) assimilation by
719 *Synechococcus* in the Gulf of Mexico and northwest Atlantic Ocean, *Limnol. Oceanogr.*, 50(6), 1924–1931,
720 doi:10.4319/lo.2005.50.6.1924, 2005.

721 Marie, D., Simon, N., and Vaulot, D.: Phytoplankton cell counting by flow cytometry, *Algal Cult. Tech.*, 253–267,
722 doi:10.1016/B978-012088426-1/50018-4, 2005.

723 Mucci, A., Levasseur, M., Gratton, Y., Martias, C., Scarratt, M., Gilbert, D., Tremblay, J.-É., Ferreyra, G., and Lansard, B.:
724 Tidally-induced variations of pH at the head of the Laurentian Channel, *Can. J. Fish. Aquat. Sci.*, doi:10.1139/cjfas-2017-
725 0007, 2017.

726 Nguyen, B. C., Belviso, S., Mihalopoulos, N., Gostan, J., Nival, P.: Dimethyl sulfide production during natural
727 phytoplankton blooms, *Mar. Chem.*, 24, 133–141, 1988

728 Nightingale, P.D., Malin, G., Law, C.S., Watson, A.J., Liss, P.S., Liddicoat, M.I., Boutin, J., Upstill-Goddard, R.C.: In situ
729 evaluation of air–sea gas exchange parameterizations using novel conservative and volatile tracers, *Global Biogeochem.*
730 *Cycles*, 14 (1), 373–387, 2000.

731 Niki, T., Kunugi, M., and Otsuki, A.: DMSP-lyase activity in five marine phytoplankton species: Its potential importance in
732 DMS production, *Mar. Biol.*, 136(5), 759–764, doi:10.1007/s002279900235, 2000.

733 Park, K. T., Lee, K., Shin, K., Yang, E. J., Hyun, B., Kim, J. M., Noh, J. H., Kim, M., Kong, B., Choi, D. H., Choi, S. J.,
734 Jang, P. G., and Jeong, H. J.: Direct linkage between dimethyl sulfide production and microzooplankton grazing, resulting
735 from prey composition change under high partial pressure of carbon dioxide conditions, *Environ. Sci. Technol.*, 48(9), 4750–
736 4756, doi:10.1021/es403351h, 2014.

737 Parsons, T. R., Maita, Y., and Lalli, C. M.: A manual of chemical and biological methods for seawater analysis, Permagon
738 Press, New York, 1984.

739 Paul, C., Sommer, U., Garzke, J., Moustaka-Gouni, M., Paul, A., and Matthiessen, B.: Effects of increased CO₂
740 concentration on nutrient limited coastal summer plankton depend on temperature, *Limnol. Oceanogr.*, 61(3), 853–868,
741 doi:10.1002/lno.10256, 2016.

742 Pierrot, D. E., Lewis, E., and Wallace, D. W. R.: MS Excel program developed for CO₂ system calculations, Carbon
743 Dioxide Information Analysis Center, ONRL/CDIAC-105a, Oak Ridge National Laboratory, US Department of Energy, Oak
744 Ridge, Tennessee, USA, 2006.

745 Pinhassi, J., Simó, R., González, J. M., Vila, M., Alonso-Sáez, L., Kiene, R. P., Moran, M. A., and Pedrós-Alió, C.:
746 Dimethylsulfoniopropionate turnover is linked to the composition and dynamics of the bacterioplankton assemblage during a
747 microcosm phytoplankton bloom, *Appl. Environ. Microbiol.*, 71(12), 7650–7660, doi:10.1128/AEM.71.12.7650-7660.2005,
748 2005.

749 Quinn, P. K., and Bates, T. S.: The case against climate regulation via oceanic phytoplankton sulphur emissions., *Nature*,
750 480(7375), 51–6, doi:10.1038/nature10580, 2011.

751 Quinn, P. K., Coffman, D. J., Johnson, J. E., Upchurch, L. M., and Bates, T. S.: Small fraction of marine cloud condensation
752 nuclei made up of sea spray aerosol, *Nat. Geosci.*, 10(9), 674–679, doi:10.1038/ngeo3003, 2017.

753 R Core Team: R: A language and environment for statistical computing. R Foundation for Statistical Computing, Vienna,
754 Austria. URL <https://www.R-project.org/>, 2016.

755 Riebesell, U. and Gattuso, J. P.: Lessons learned from ocean acidification research, *Nat. Clim. Chang.*, 5(1), 12–14,
756 doi:10.1038/nclimate2456, 2015.

757 Robert-Baldo, G., Morris, M., and Byrne, R.: Spectrophotometric determination of seawater pH using phenol red, *Anal.*
758 *Chem.*, 3(57), 2564–2567, doi:10.1021/ac00290a030, 1985.

759 Roemmich, D., Church, J., Gilson, J., Monselesan, D., Sutton, P. and Wijffels, S.: Unabated planetary warming and its ocean
760 structure since 2006, *Nat. Clim. Chang.*, 5(3), 240–245, doi:10.1038/nclimate2513, 2015.

761 Ruiz-González, C., Galí, M., Gasol, J. M. and Simó, R.: Sunlight effects on the DMSP-sulfur and leucine assimilation
762 activities of polar heterotrophic bacterioplankton, *Biogeochemistry*, 110(1–3), 57–74, doi:10.1007/s10533-012-9699-y,
763 2012.

764 Scarratt, M. G., Levasseur, M., Schultes, S., Michaud, S., Cantin, G., Vézina, A., Gosselin, M. and De Mora, S. J.:
765 Production and consumption of dimethylsulfide (DMS) in North Atlantic waters, *Mar. Ecol. Prog. Ser.*, 204, 13–26,
766 doi:10.3354/meps204013, 2000.

767 Schlüter, L., Lohbeck, K. T., Gröger, J. P., Riebesell, U. and Reusch, T. B. H.: Long-term dynamics of adaptive evolution in
768 a globally important phytoplankton species to ocean acidification, *Sci. Adv.*, 2(7), e1501660–e1501660,
769 doi:10.1126/sciadv.1501660, 2016.

770 Schwinger, J., Tjiputra, J., Goris, N., Six, K. D., Kirkevåg, A., Seland, Ø., Heinze, C. and Ilyina, T.: Amplification of global
771 warming through pH dependence of DMS production simulated with a fully coupled Earth system model, *Biogeosciences*,
772 14(15), 3633–3648, doi:10.5194/bg-14-3633-2017, 2017.

773 Simó, R.: Production of atmospheric sulfur by oceanic plankton: Biogeochemical, ecological and evolutionary links, Trends
774 Ecol. Evol., 16(6), 287–294, doi:10.1016/S0169-5347(01)02152-8, 2001.

775 Simó, R.: From cells to globe: approaching the dynamics of DMS(P) in the ocean at multiple scales, Can. J. Fish. Aquat.
776 Sci., 61(5), 673–684, doi:10.1139/f04-030, 2004.

777 Simó, R., and Pedrós- Alió, C.: Role of vertical mixing in controlling the oceanic production of dimethyl sulphide, Nature,
778 402, 396–399, doi:10.1038/46516, 1999.

779 Six, K. D., Kloster, S., Ilyina, T., Archer, S. D., Zhang, K., and Maier-Reimer, E.: Global warming amplified by reduced
780 sulphur fluxes as a result of ocean acidification, Nat. Clim. Chang., 3(11), 975–978, doi:10.1038/nclimate1981, 2013.

781 Starr, M., St-Amand, L., Devine, L., Bérard-Therriault, L. and Galbraith, P. S.: State of phytoplankton in the Estuary and
782 Gulf of St. Lawrence during 2003, CSAS Res. Doc., 2004/123, 35, 2004.

783 Stefels, J.: Physiological aspects of the production and conversion of DMSP in marine algae and higher plants, J. Sea Res.,
784 43(3–4), 183–197, doi:10.1016/S1385-1101(00)00030-7, 2000.

785 Stefels, J., and Van Boekel, W. H. M.: Production of DMS from dissolved DMSP in axenic cultures of the marine
786 phytoplankton species *Phaeocystis* sp., Mar. Ecol. Prog. Ser., 97(1), 11–18, doi:10.3354/meps097011, 1993.

787 Stefels, J., Steinke, M., Turner, S., Malin, G., and Belviso, S.: Environmental constraints on the production and removal of
788 the climatically active gas dimethylsulphide (DMS) and implications for ecosystem modelling, Biogeochemistry, 83(1–3),
789 245–275, doi:10.1007/s10533-007-9091-5, 2007.

790 Steinke, M., Malin, G., Archer, S. D., Burkill, P. H. and Liss, P. S.: DMS production in a coccolithophorid bloom: Evidence
791 for the importance of dinoflagellate DMSP lyases, Aquat. Microb. Ecol., 26(3), 259–270, doi:10.3354/ame026259, 2002.

792 Stillman, J. H. and Paganini, A. W.: Biochemical adaptation to ocean acidification, J. Exp. Biol., 218(12), 1946–1955,
793 doi:10.1242/jeb.115584, 2015.

794 Sunda, W., Kieber, D. J., Kiene, R. P., and Huntsman, S.: An antioxidant function for DMSP and DMS in marine algae,
795 Nature, 418(6895), 317–320, 2002.

796 Toole, D. A., and Siegel, D. A.: Light-driven cycling of dimethylsulphide (DMS) in the Sargasso Sea: closing the loop,
797 Geophys. Res. Lett., 31(9), 1–4, doi:10.1029/2004GL019581, 2004.

798 Toole, D. A., Slezak, D., Kiene, R. P., Kieber, D. J., and Siegel, D. A.: Effects of solar radiation on dimethylsulphide cycling
799 in the western Atlantic Ocean, Deep. Res. Part I Oceanogr. Res. Pap., 53(1), 136–153, doi:10.1016/j.dsr.2005.09.003, 2006.

800 Toole, D. A., Siegel, D. A. and Doney, S. C.: A light-driven, one-dimensional dimethylsulphide biogeochemical cycling
801 model for the Sargasso Sea, J. Geophys. Res. Biogeosciences, 113(2), 1–20, doi:10.1029/2007JG000426, 2008.

802 Vallina, S. M., Simó, R., Anderson, T. R., Gabric, A., Cropp, R., and Pacheco, J. M.: A dynamic model of oceanic sulfur
803 (DMOS) applied to the Sargasso Sea: Simulating the dimethylsulphide (DMS) summer paradox, J. Geophys. Res.
804 Biogeosciences, 113(1), doi:10.1029/2007JG000415, 2008.

805 Vila, M., Simó, R., Kiene, R. P., Pinhassi, J., González, J. M., Moran, M. A., and Pedrós-Alió, C.: Use of
806 microautoradiography combined with fluorescence in situ hybridization to determine dimethylsulfoniopropionate

807 incorporation by marine bacterioplankton taxa, *Appl. Environ. Microbiol.*, 70, 4648– 4657,
808 <https://doi.org/10.1128/AEM.70.8.4648-4657.2004>, 2004.

809 Vila-Costa, M., Simó, R., Harada, H., Gasol, J. M., Slezak, D., and Kiene, R. P.: Dimethylsulfoniopropionate Uptake by
810 Marine Phytoplankton, *Science*, 314, 652–654, 2006a.

811 Vila-Costa, M., Del Valle, D. A., González, J. M., Slezak, D., Kiene, R. P., Sánchez, O., and Simó, R.: Phylogenetic
812 identification and metabolism of marine dimethylsulfide consuming bacteria, *Environ. Microbiol.*, 8, 2189–2200,
813 <https://doi.org/10.1111/j.1462-2920.2006.01102.x>, 2006b.

814 Vila-Costa, M., Pinhassi, J., Alonso, C., Pernthaler, J., and Simó, R.: An annual cycle of dimethylsulfoniopropionate sulfur
815 and leucine assimilating bacterioplankton in the coastal NW Mediterranean, *Environ. Microbiol.*, 9, 2451–2463,
816 <https://doi.org/10.1111/j.1462-2920.2007.01363.x>, 2007.

817 Vogt, M., Steinke, M., Turner, S., Paulino, a., Meyerhöfer, M., Riebesell, U., Le Quéré, C. and Liss, P.: Dynamics of
818 dimethylsulphoniopropionate and dimethylsulphide under different CO₂ concentrations during a mesocosm experiment,
819 *Biogeosciences*, 5(2), 407–419, doi:10.5194/bg-5-407-2008, 2008.

820 Webb, A., Malin, G., Hopkins, F., Ho, K. L., Riebesell, U., Schulz, K., Larsen, A., and Liss, P.: Ocean acidification has
821 different effects on the production of DMS and DMSP measured in cultures of *Emiliana huxleyi* and a mesocosm study: a
822 comparison of laboratory monocultures and community interactions, *Environ. Chem.*, 13(2), 314–329,
823 doi:10.1071/EN14268, 2015.

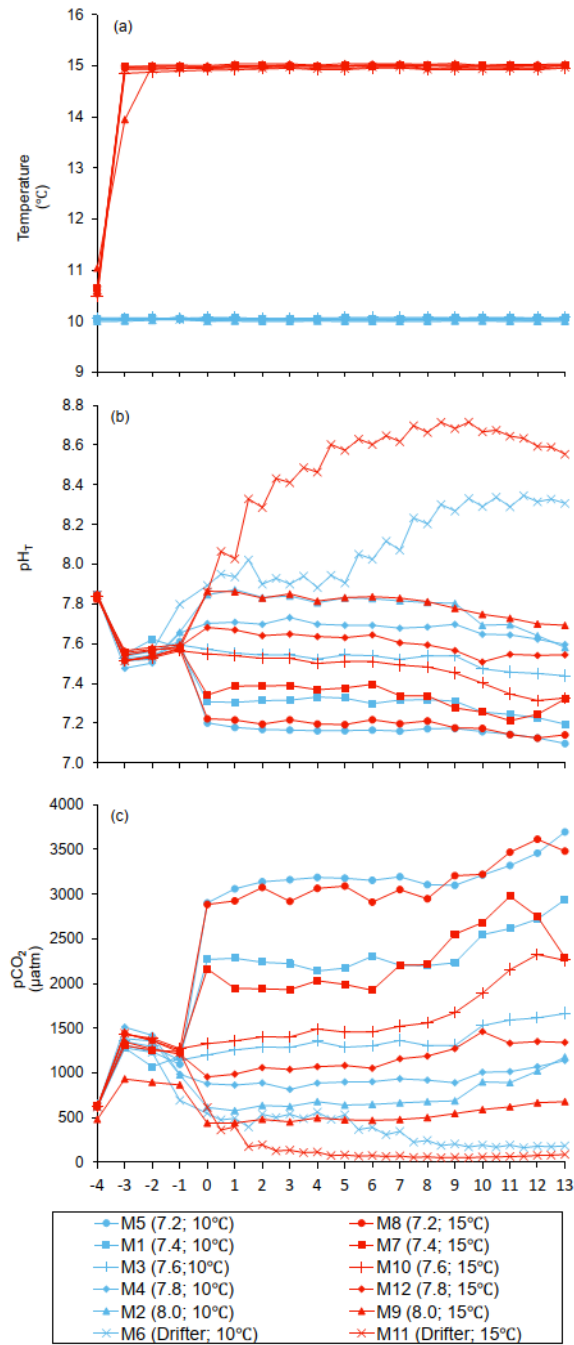
824 Webb, A. L., Leedham-Elvidge, E., Hughes, C., Hopkins, F. E., Malin, G., Bach, L. T., Schulz, K., Crawford, K., Brussaard,
825 C. P. D., Stuhr, A., Riebesell, U., and Liss, P. S.: Effect of ocean acidification and elevated *f*CO₂ on trace gas production by
826 a Baltic Sea summer phytoplankton community, *Biogeosciences*, 13(15), 4595–4613, doi:10.5194/bg-13-4595-2016, 2016.

827 Wolfe, G. V., and Steinke, M.: Grazing-activated production of dimethyl sulfide (DMS) by two clones of *Emiliana huxleyi*,
828 *Limnol. Oceanogr.*, 41(6), 1151–1160, doi:10.4319/lo.1996.41.6.1151, 1996.

829 Woodhouse, M. T., Mann, G. W., Carslaw, K. S., and Boucher, O.: Sensitivity of cloud condensation nuclei to regional
830 changes in dimethyl-sulphide emissions, *Atmos. Chem. Phys.*, 13(5), 2723–2733, doi:10.5194/acp-13-2723-2013, 2013.

831 Yoch, D. C.: Dimethylsulfoniopropionate: Its sources, role in the marine food web, and biological degradation to
832 dimethylsulfide, *Appl. Environ. Microbiol.*, 68(12), 5804–5815, doi:10.1128/AEM.68.12.5804-5815.2002, 2002.

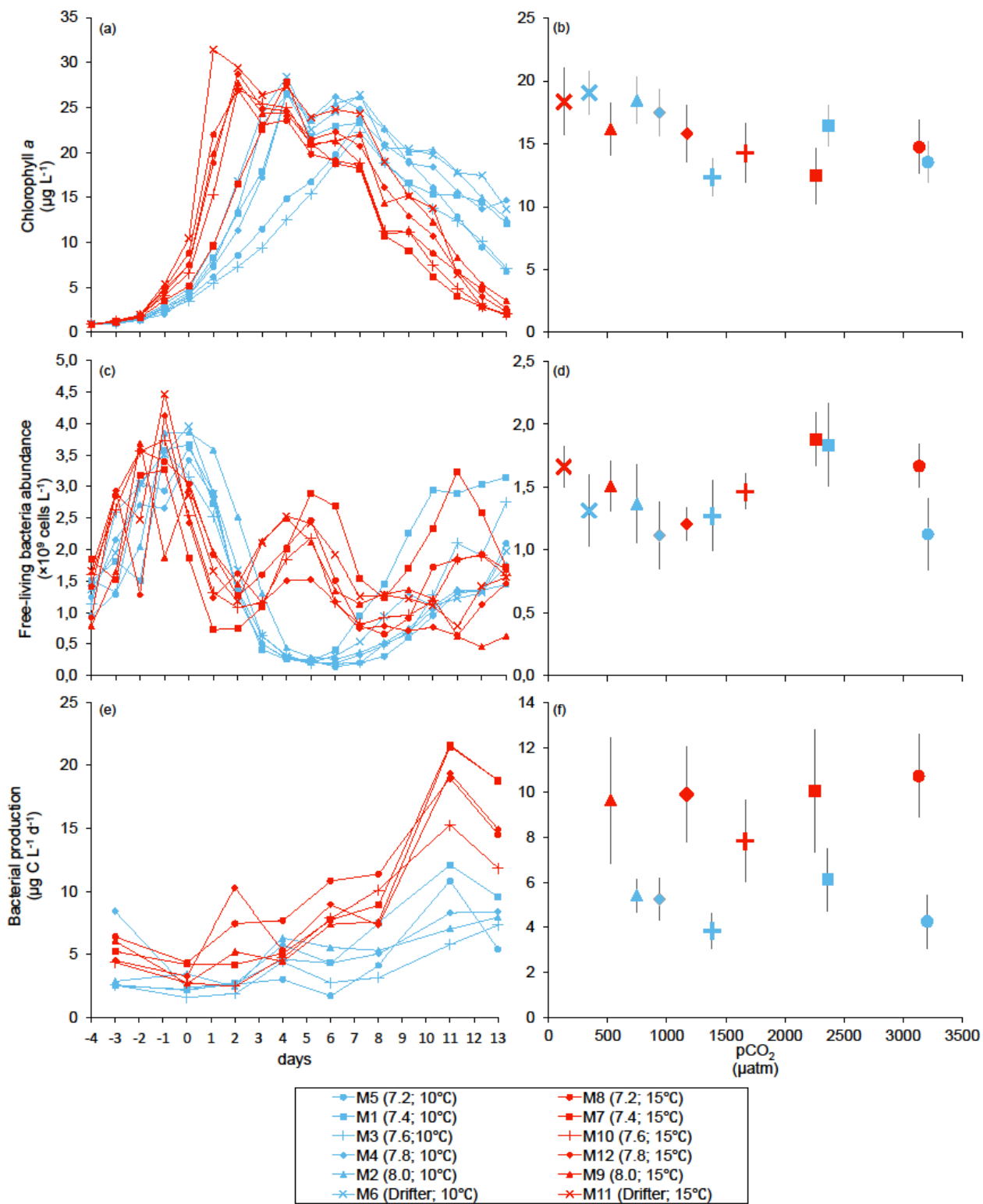
833



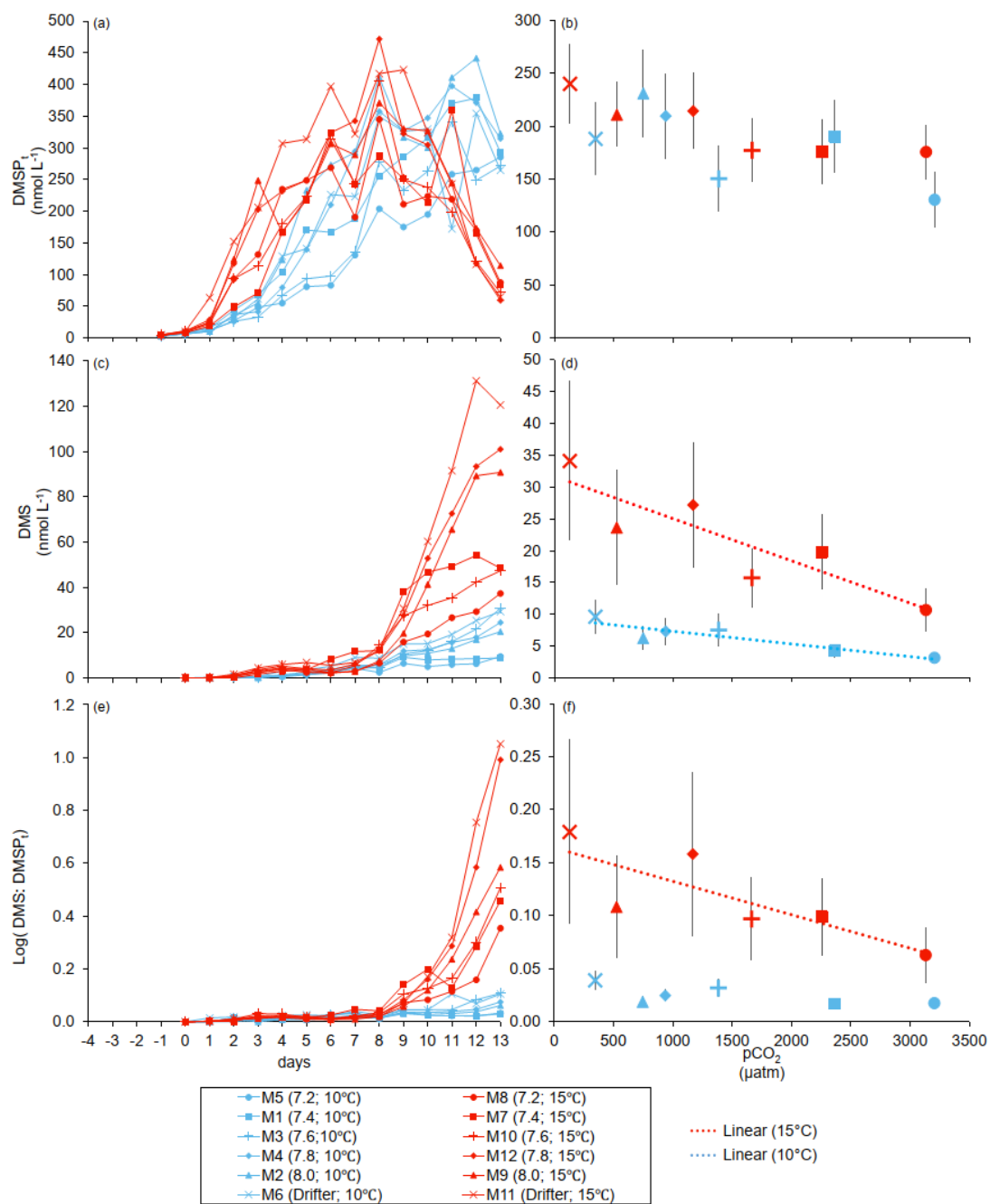
834

835 **Figure 1. Temporal variations over the course of the experiment for: (a) temperature, (b) pH_T, (c) pCO₂. For symbol attribution to**
 836 **treatments, see legend. Adapted from B nard et al. (2018).**

837



839 **Figure 2. Temporal variations, and averages over the course of the experiment (day 0 to day 13) for: (a–b) chlorophyll *a* (adapted**
840 **from B nard et al., 2018), (c–d) free-living bacteria abundance, (e–f) bacterial production. For symbol attribution to treatments,**
841 **see legend.**

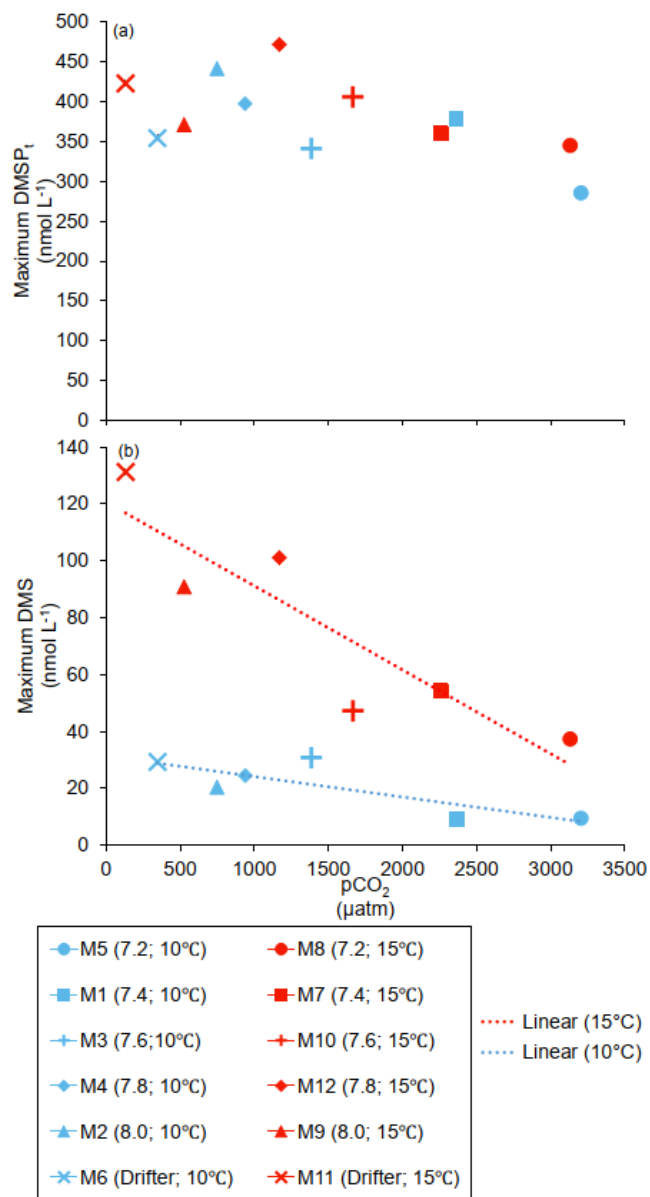


842

843

844

Figure 3. Temporal variations, and averages over the course of the experiment (day 0 to day 13) for: (a–b) DMSP₁, (c–d) DMS, (e–f) the natural logarithm of the DMS:DMSP₁ ratio. For symbol attribution to treatments, see legend.

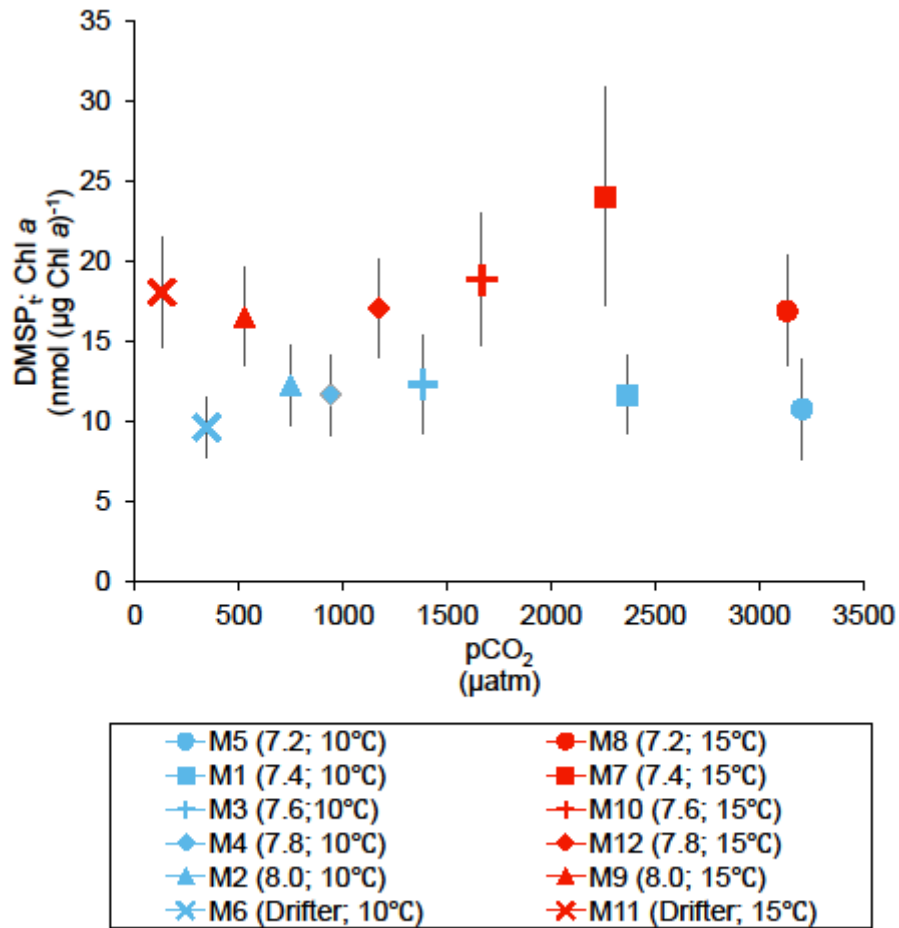


845

846

847

Figure 4. Maximum concentrations reached over the course of the experiment for: (a) DMSP_t, and (b) DMS. For symbol attribution to treatments, see legend.

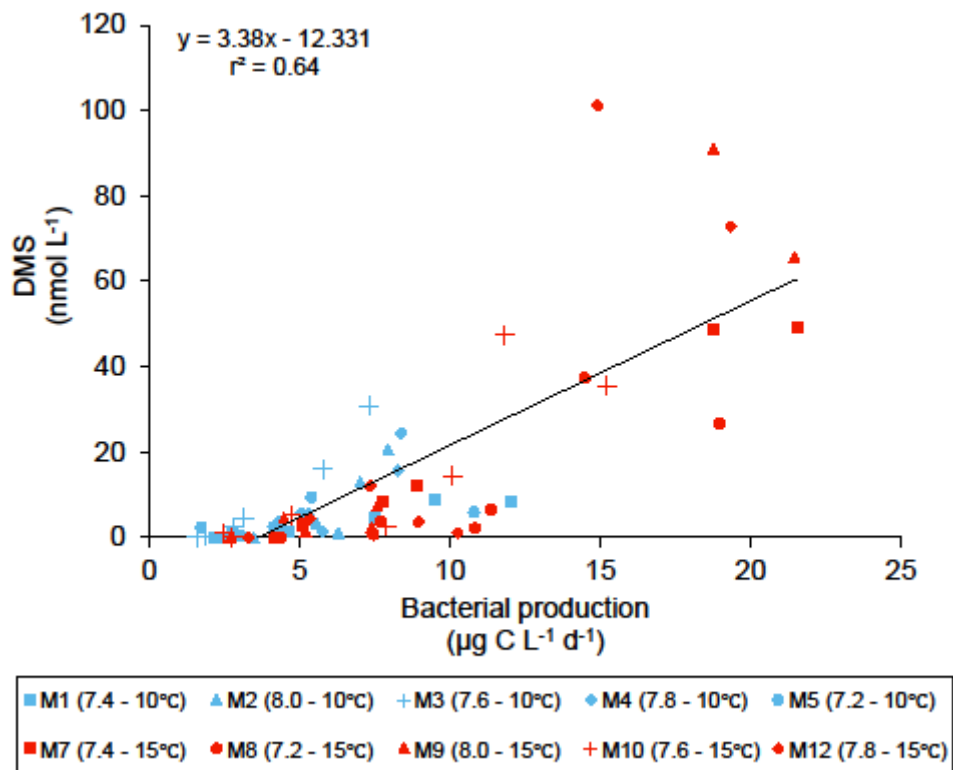


848

849

850

Figure 5. Averages of DMSP:Chl *a* ratio over the course of the experiment (day 0 to day 13). For symbol attribution to treatments, see legend.



851

852 **Figure 6. Linear regression between DMS concentrations and bacterial production during the experiment.**

853

854

855 **Table 1. Results of the generalized least squares models (gls) tests for the effects of temperature, pCO₂, and their interaction over**
 856 **the duration of the experiment (day 0 to day 13). Separate analyses with pCO₂ as a continuous factor were performed when**
 857 **temperature had a significant effect. Averages of bacterial abundance and production, DMSP_t, DMS, Chl *a*-normalized DMSP_t**
 858 **and DMS concentrations, and DMS:DMSP_t ratios are presented. Natural logarithm transformation is indicated when necessary.**
 859 **Significant results are in bold. *p<0.05, **p<0.01, ***p<0.001.**

860

| Response Variable | Factor | df | t-value | p-value |
|---|--------------------------------|----|---------------|---------------------|
| Free-living bacterial abundance ($\times 10^9$ cells L ⁻¹) | Temperature | 8 | 0.635 | 0.543 |
| | pCO ₂ | 8 | -0.083 | 0.936 |
| | pCO ₂ x Temperature | 8 | 0.221 | 0.830 |
| Bacterial production ($\mu\text{g C L}^{-1} \text{d}^{-1}$) | Temperature | 6 | 2.454 | 0.050* |
| | pCO ₂ (10°C) | 3 | -0.272 | 0.803 |
| | pCO ₂ (15°C) | 3 | 0.746 | 0.510 |
| DMSP _t (nmol L ⁻¹) | Temperature | 8 | 0.509 | 0.625 |
| | pCO ₂ | 8 | -0.767 | 0.465 |
| | pCO ₂ x Temperature | 8 | 0.134 | 0.897 |
| DMS (nmol L ⁻¹) | Temperature | 8 | 6.822 | <0.001*** |
| | pCO ₂ (10°C) | 4 | -4.483 | 0.011* |
| | pCO ₂ (15°C) | 4 | -3.799 | 0.019* |
| DMSP _t :Chl <i>a</i> ratio (nmol ($\mu\text{g Chl } a$) ⁻¹) | Temperature | 8 | 2.627 | 0.030* |
| | pCO ₂ | 8 | 0.123 | 0.908 |
| | pCO ₂ x Temperature | 8 | 0.621 | 0.568 |
| DMS:Chl <i>a</i> ratio (nmol ($\mu\text{g Chl } a$) ⁻¹) | Temperature | 8 | 5.225 | <0.001*** |
| | pCO ₂ (10°C) | 4 | -1.373 | 0.242 |
| | pCO ₂ (15°C) | 4 | -2.227 | 0.090 |
| Log(DMS:DMSP _t) | Temperature | 8 | 5.131 | <0.001*** |
| | pCO ₂ (10°C) | 4 | -1.844 | 0.139 |
| | pCO ₂ (15°C) | 4 | -3.138 | 0.035* |

861

862

863 **Table 2. Results of the generalized least squares models (gls) tests for the effects of temperature, pCO₂, and their interaction on the**
 864 **maximum values of the parameters measured during the experiment. Separate analyses with pCO₂ as a continuous factor were**
 865 **performed when temperature had a significant effect. Maxima of DMSP_t, and DMS concentrations are presented. Significant**
 866 **results are in bold. *p<0.05, **p<0.01, ***p<0.001.**

867

| Response Variable | Factor | df | t-value | p-value |
|--|--------------------------------|----|---------------|---------------------|
| DMSP _t (nmol L ⁻¹) | Temperature | 8 | 0.384 | 0.711 |
| | pCO ₂ | 8 | -0.713 | 0.496 |
| | pCO ₂ x Temperature | 8 | 0.300 | 0.772 |
| DMS (nmol L ⁻¹) | Temperature | 8 | 6.403 | <0.001*** |
| | pCO ₂ (10°C) | 4 | -2.868 | 0.046* |
| | pCO ₂ (15°C) | 4 | -4.061 | 0.015* |

868